1972

Test of a fully-welded beam-to-column connection, September 1972 (73-48) PB 234 401/AS

John E. Regec

Joseph S. Huang

Wai-Fah Chen

OFFICE
OF
RESEARCH

LEHIGH UNIVERSITY

Beam-to-Column Connections

TEST OF A FULLY-WELDED BEAM-TO-COLUMN CONNECTION

by

John E. Regec

Joseph S. Huang

Wai-Fah Chen

Fritz Engineering Laboratory Report No. 333.21

Beam-to-Column Connections

TEST OF A FULLY-WELDED BEAM-TO-COLUMN CONNECTION

by

John E. Regec

Joseph S. Huang

Wai-Fah Chen

This work has been carried out as part of an investigation sponsored jointly by the American Iron and Steel Institute and the Welding Research Council.

Department of Civil Engineering

Fritz Engineering Laboratory
Lehigh University
Bethlehem, Pennsylvania

September 1972

Fritz Engineering Laboratory Report No. 333.21

TABLE OF CONTENTS

		Page
	ABSTRACT	1
1.	INTRODUCTION	2
	1.1 Summary of Previous Research	2
	1.2 Objective of This Study	3
2.	DEVELOPMENT OF TEST	5
	2.1 Preliminary Analysis	5
	2.2 Connection Design	5
3.	TEST PROGRAM	7
	3.1 Description of Connection	7
	3.2 Material Properties	7
	3.3 Test Setup	7
	3.4 Instrumentation	8
4.	TEST RESULTS AND DISCUSSION	9
	4.1 Test Procedure and Observations	9
	4.2 Discussion of Results	10
	4.2.1 Column Behavior	11
	4.2.2 Beam Behavior	12
	4.2.3 Beam-to-Column Interaction	14
5.	SUMMARY AND CONCLUSIONS	16
6.	ACKNOWLEDGMENTS	17
7.	APPENDICES	18
	7.1 Design of Connection C12	18
	7.2 Stress-Strain Relationship	21
8.	FIGURES	24
9.	REFERENCES	47

LIST OF FIGURES

Figure		Page
1	Moment-rotation curves	24
2	Test C12 detail	25
3	General instrumentation	26
4	Panel zone instrumentation	27
5	Load-deflection curve	28
6	Fracture of weld at tension flange	29
7	Fracture of weld along beam web	30
8	Connection at end of test	31
9	Variation of vertical stress along column innerface (k-line)	32
10	Variation of horizontal stress along column innerface (k-line)	33
11	Variation of horizontal stress along column centerline	34
12	Panel stress field at 425 K load	35
13	Panel stress field at 520 K load	36
14	Panel stress field at 680 K load	37
15	Panel stress field at 750 K load	38
16	Maximum shear stress variation in column web	39
17	Variation of stress across beam flanges adjacent to column	40
18	Stress variation along beam depth adjacent to column flange	41
19	Beam stress variation--predicted versus actual	42
20	Beam shear stress variation with load at section D-D	43
21	Bending moment diagram	44
22	Sequence of panel zone yielding	45
23	Load-rotation curve	46

A B S T R A C T

A test program has been developed which has the objective of investigating various symmetrically-loaded moment-resisting beam-to-column connections which are of extreme importance in design and construction of steel multi-story frames. This report covers the testing of the first in a series of twelve specimens--a fully-welded beam-to-column connection.

In this report the design procedure is presented which forms the basis for this testing series. The test procedure is given along with a step-by-step description and analysis of the stress patterns in the section.

It was found that this type of connection can be used in plastic design as adequate stiffness in the elastic range was developed along with sufficient strength and rotation capacity. The AISC Specification provided adequate rules in design of such a welded connection.

The initial cause of unloading was buckling of column web in the compression region. Testing was concluded due to a combination of excessive column web deformation and cracking at the tension flange weld. The weld did not fail but pulled out the surrounding column flange material.

This report should provide a basis for studying the behavior of the remaining tests in this series. It is hoped that results of this and the eleven other connections will furnish adequate information so that more efficient and economical designs can be made.

1. INTRODUCTION

In the construction of steel multi-story building frames, one of the most important components affecting costs is the moment-resisting beam-to-column connections. The designer faces the decision of whether to choose bolted joints, welded joints, or combinations of both for certain construction situations. Both economy and ease of erection play an important part in determining which type of connection is to be used.

Reference 7 summarizes several types of connections which are commonly used in construction and are of particular interest to designers. This reference is an interim report prepared to indicate areas of future research needs in beam-to-column connections.

1.1 SUMMARY OF PREVIOUS RESEARCH

Research on moment-resisting beam-to-column connections has been conducted at Cambridge University, Cornell University, and Lehigh University. These results are summarized and discussed in Ref. 3. The types of connections studied are: fully welded connections, welded top plate and angle seat connections, bolted top plate and angle seat connections, end plate connections, and T-stub connections. In addition, the behavior of welded corner connections, bolted lap splices in beams, and end plate type beam splices was discussed. The connecting media for these specimens were welding, riveting, and bolting. Only A325 high-strength bolts were used. The most important result of these tests is that for all properly designed and detailed welded and bolted moment

connections the plastic moment of the adjoining member was reached, and the connections were able to develop large plastic rotation capacity. There were no premature failures except those which could have been predicted and prevented.[3]

Recently, a series of eight tests of full-size steel beam-to-column connections was carried out at the University of California.[9] The connections were subjected to cyclic loading simulating earthquake effects on a building frame. Among those connections tested were two fully welded connections, five flange-welded web-bolted connections, and one flange-welded connection. A325 bolts were used in fastening the web shear plates. Beam sections used were W18x50 and W24x76; column sections were W12x106. The connection specimens were made of ASTM A36 steel. All connections had horizontal stiffeners which were connected to the columns by groove welds. Results of this series of tests show that the hysteresis loops in all cases were stable in shape under repeated loading cycles. The failure of connections was due to either local buckling of beam flanges or weld fracture, and occurred only after many cycles of loading beyond yield.

1.2 OBJECTIVE OF THIS STUDY

Presently, at Lehigh University a research project is being undertaken with the purpose of investigating the performance of various welded and/or bolted beam-to-column connections which are of high importance in design and construction of steel building frames. Reference 6 gives a detailed description of that test program.

The present study concerns the first connection of the test series (Test C12 of Ref. 6). This specimen is fully welded and serves as a control specimen for the purpose of evaluating the performance of several other connections of different joint design in the series.

Herein, the load-deformation behavior of this control connection is presented. Stress fields throughout the system are reported at various loads. Deflections and rotations of the structure along with the moment capacity and overall stiffness of the connection are studied.

2. DEVELOPMENT OF TEST

2.1 PRELIMINARY ANALYSIS

The connection used in this test (along with all others in the test series) is designed according to plastic analysis procedures. In Fig. 1 the behavior of a beam-to-column connection under symmetric loading is schematically illustrated in a moment-rotation curve. By properly designing the joint and preventing possible premature failure, the connection will be able to carry the plastic moment of the beam with sufficient rotation capacity and overall stiffness, as indicated by Curve A. However, if the design is unsatisfactory, the connection behavior will not be adequate. This is depicted by Curves B, C. and D. The connection tested is proportioned so that Curve A can be obtained.

2.2 CONNECTION DESIGN

The specimen is designed according to the AISC Specification.[1] The loading condition for this test attempted to simulate gravity type loading (dead load plus live load). The load factor used was then 1.7. The connection, along with all others in the series, was designed so that it could resist the plastic moment of the beam section.

The connection was chosen in such a beam and column combination so that it represented a real interior beam-to-column connection in a multi-story frame.

The column section chosen was that which had the least size permitted without requiring horizontal stiffeners (according to AISC Specification). The specimen was proportioned in such a way that at

beam-to-column juncture the plastic moment and factored shear capacity would be reached simultaneously. This connection (C12) was designed along with four others of the same size. All five were designed to resist the same moment and shear. Test C2 (see Ref. 6) was designed using a shear plate attached with A490 bolts. The allowable shear stress used in design for A490 bolts is 40 ksi.[5] The shear capacity of these bolts is 374 kips, which is about 94.7% of V_p of the section. To compare the behavior of all five connections, the remaining specimens, including C12, were then designed using a 374 kip shear capacity. Beam span was then calculated as the ratio of moment to shear.

The sections used in this connection are a W27x94 beam and a W14x176 column. The material used is ASTM A572 Gr. 55 steel.

The specimen was welded according to the AWS Building Code.[2] The welding process used was innershield procedure; the electrodes were E70TG (flux cored arc welding with no auxiliary gas shielding). The types of filler metal for beam flange groove welds and beam web groove welds are NR311 and NR202, respectively. All groove welds were inspected by ultrasonic testing as per AWS Code. The detailed design procedure for Test C12 is presented in Appendix 1.

3. TEST PROGRAM

3.1 DESCRIPTION OF CONNECTION

The joint detail of specimen C12 is shown in Fig. 2. The beam flanges and beam web are connected to the column flanges by groove welds. To simulate actual field practices, an erection plate is tack welded to the column flange. A307 erection bolts are used as temporary attachments of beam to column during the welding process. The erection plate also serves as a backing strip for the beam web groove weld.

3.2 MATERIAL PROPERTIES

The material used for both beam and column is ASTM A572 Grade 55 steel. Properties used in determining stresses are as follows:

Modulus of elasticity (E) = 29,570 ksi

Yield strain (ε_y) = 0.001857 in./in.

Yield stress (σ_y) = 54.9 ksi

Strain at onset of strain hardening (ε_{st}) = 0.0150 in./in.

Strain hardening modulus (E_{st}) = 581 ksi

A detailed report of material properties is included in Ref. 10.

3.3 TEST SETUP

The test setup is shown in Fig. 3. A 5,000,000 pound-capacity hydraulic testing machine was used to apply axial load in the column. The beams were supported by two pedestals resting on the floor. Rollers were used to simulate simply supported end conditions. Because of the size of sections and the short span of the beam used, no lateral bracing was needed to provide stability. Bearing stiffeners were provided over supports to insure no web crippling would occur in the beam.

3.4 INSTRUMENTATION

Figure 3 gives an overall view of the instrumentation used for analysis in this report. Gages were placed on beam flanges to determine the moment diagram of the beam and to provide checks for possible lateral buckling. Additional SR-4 gages were placed at sections C-C and D-D for determining stress distribution in beam flanges. Gages were also attached at section G-G in the column and were used to align the connection and testing machine crosshead. Dial gages were located directly under the column for measuring overall deflection and in the column web compression region for determining web buckling. Level bars were attached near beam-to-column juncture to determine the rotation capacity of the joint.

In Fig. 4 the panel zone instrumentation is shown. Gages were provided in the beam web to obtain the stress distribution throughout this section. The gages in the column web panel zone were placed to provide the general stress distribution and flow throughout the zone. Gages A, C, G, and I were placed at a distance of $\frac{1}{2}$ (t_b + 5k) from beam flange centerline. (In the present AISC Specification,[1] formula (1.15-1), which pertains to requirements for stiffening in the compression region, was developed from the concept that the column flange acts as a bearing plate. It distributes the load caused by the beam compression flange to the column web with a width of t_b + 5k.) The information from these, along with that in later tests, should provide data for determining the validity of present assumptions of stress distribution. All gages shown along the column innerface were placed at the toe of fillet. Strain rosettes K were placed on opposite sides at the same location. These values were averaged to account for any early web buckling.

4. TEST RESULTS AND DISCUSSION

As described in Section 2.2, this connection is to simulate an actual interior symmetrically-loaded beam-to-column connection in a multi-story building frame. The test setup of Fig. 3 shows the connection in an inverted position.

4.1 TEST PROCEDURE AND OBSERVATIONS

The applied load was increased continuously until failure. After each load increment, all gage readings were recorded. Vertical alignment was checked after each loading by means of a transit to insure no development of possible lateral buckling. Points of a load-deflection curve were plotted continuously so that general specimen behavior could be observed and further load increments adjusted.

The load-deflection curve of Test C12 is shown in Fig. 5. Load increments of 25 kips were used initially. At an applied load of 475 kips the first yield lines began forming in the compression web of the column. Both localized yielding at the toe of fillet and yielding at the web center (between beam compression flanges) were observed. At this point the load-deflection curve began to deviate from the linear. At 600 kips yielding was observed in the tension region of the column web near toe of fillet. By this load the yielded region appeared to extend completely through the compression zone of the web. Yielding in the upper beam web near the compression flange was also observed. Load increments of about 20 kips were applied until a 680 kip load was reached. The specimen was then unloaded to complete the

first cycle of testing, as shown in Fig. 5. A small load was kept on the specimen between cycles to insure no alignment change.

On the second loading cycle after reloading to 680 kips, additional loading was continued at the same rate until at 700 kips increments were changed from a load rate to a specified deflection rate. The load was allowed to stabilize until there was no further movement of the sensitive crosshead, with the loading value closed.

During the third cycle at a load of 768 kips buckling of the compression web began (see Fig. 5 for web buckling curve). The connection attained a maximum load of 838 kips at a deflection of approximately 2.7 in. At this point compression web buckling was very large as seen from Fig. 5. Deflection increments were increased to 0.20 in. until end of test. Testing was concluded due to a combination of excessive column web deformation and fracture of weld at tension flange and along beam web. Figure 6 shows a view of the fracture of weld at the tension flange. As seen by the picture, the weld did not fail but pulled out the surrounding column flange material. Figure 7 shows ripping of the beam which occurred simultaneously. The connection at conclusion of testing is shown in Fig. 8.

4.2 DISCUSSION OF RESULTS

Methods for determining the state of stresses and yielding from strain gage readings are presented in Appendix 2.

Data reduction is broken down into three major parts--column behavior, beam behavior, and beam-to-column interaction.

4.2.1 Column Behavior

Figure 9 shows the variation of the vertical stress (σ_y) along the column innerface (k-line). The vertical stresses are seen to be compressive in the upper region but become tensile as the lower, tension region is approached. Along the beam centerline, vertical stress was found to be very small (less than 7 ksi) up to the working load of approximately 450 kips. All stresses were compressive.

Variation of horizontal stress (σ_x) along the column innerface (k-line) is shown in Fig. 10. Slightly below working load initial yielding was observed at rosette B. At a load of 475 kips yielding occurred at gage H in the web tension region innerface. As seen in Fig. 10 when yielding was recorded at a gage, it was assumed that the point remained at the yield stress and that further loading increments did not affect the stress. Results of tensile tests[10] form the basis for this assumption as it was found that after yielding the material exhibited an extensive yield plateau before strain hardening occurred.

The horizontal stress variation along column centerline is nearly linear and approximately zero at centerline intersection, as shown in Fig. 11. However, the linearity does not remain at higher loads as yielding occurs at the compression rosette at 520 kips and not before 768 kips at the tension gage.

Figures 12 to 15 show the principal stresses in the panel zone region at various loads (refer to Fig. 5 for location on load-deflection curve). Gages directly across from the beam flanges have maximum principal stresses only slightly higher than the horizontal

stresses. The direction of these principal stresses in both the compression and tension web area varied usually not more than 15^{o} from horizontal. As working load was approached this variation was not more than 9^{o}. At the column center the maximum principal stress can be assumed to act horizontal.

Figure 16 shows plots of applied load versus maximum shear stress in column web rosettes, as determined by Mohr's circle. Solid lines show variation in center rosettes, and dashed lines represent variation at corresponding innerface rosettes. As seen in the first and third plots, the maximum shear is nearly the same in the compression and tension regions up to a 425 kip applied load. The curve of gage K changes drastically at this point. This effect is probably caused by yielding near that region as exhibited by yielding in the adjacent rosette.

The center plot shows variation in the gages at the panel center region. Up to working load the maximum shear at column innerface is about twice that at centerline.

4.2.2 Beam Behavior

Flange stress variation near beam-to-column juncture is shown in Fig. 17. The center gage of the lower right flange was not functioning so that the flange distribution of this section was incomplete. Initial yielding in the connection occurred at gage S at a load of 425 kips (see Fig. 3 for location). Both tension flanges fully yielded at an applied load of about 65 kips less than that causing full yielding

in the compression flanges. This difference is attributed to the existence of residual stresses in rolled shapes. Figure 17 reflects that actual flange stress distribution approaches a parabolic shape rather than the assumed uniform distribution.

Strain hardening in the flanges first occurred at a load of 703 kips. Gages U, W, and T began strain hardening at this load (see Fig. 3). All flanges were fully strain hardened between 705 and 724 kips. The load-deflection curve of Fig. 5 reflects this occurrence as at a load of 703 kips instead of continuing to level off, the curve begins to rise.

Figure 18 shows the variation of horizontal stress throughout a beam section located at a distance of two inches from the column flange. Although the distribution is nearly linear, a comparison with the theoretical distribution in Fig. 19 shows that near working load the actual stresses are much higher, especially in the flange region.

Shear stress in the beam web was measured by a rosette P. Shear stress (τ_{xy}) and maximum shear stress were almost exactly the same. Figure 20 shows a plot of load versus shear stress (or maximum shear stress). A bilinear relationship is observed either side of the working load.

The bending moment diagrams of the beam sections at various loads are shown in Fig. 21. Predicted moments (dashed lines) agree closely with actual results at various beam locations except near beam-to-column juncture. This discrepancy is probably due to the effect

of residual stresses from welding which are causing work hardening in the material.

4.2.3 Beam-to-Column Interaction

The panel stress field and adjacent beam stresses are shown in Figs. 12 to 15. As the load-deflection curve begins to deviate from linearity (see Fig. 5), panel zone points near flange juncture along with beam flanges begin to yield as shown in Fig. 13. As the load increased, yielding progressed toward the center region of panel zone and beam web. Figure 14 shows the stress distribution at a 680 kip applied load. Shear yielding began at beam web center at 660 kips. With these regions yielded, deflection of the specimen increased at a much higher rate compared to applied load, as evidenced in Fig. 5. Figure 15 shows the stress field at plastic limit load (P_p). Strain hardening occurred in the beam flanges which helped the connection attain P_p instead of levelling off at a plateau below this load. By this time yielding spread such that gages at a distance $\frac{1}{2}$ (t_b + 5k) from beam flange centerline also yielded. A summary of the yielding sequence along with the governing type of stress is provided in Fig. 22.

The specimen continued to deform with buckling in the compression zone beginning at about 768 kips. Figure 5 shows a plot of load versus lateral deflection in the compression zone. This led to the combined cause of failure of column web buckling and fracture of weld at the tension flange.

From the load-deflection curve of Fig. 5, it can be seen that the AISC Specification[1] is adequate for design of this connection.

Sufficient stiffness was exhibited in the elastic range, and the desired strength and rotation capacity were attained. Web buckling occurred slightly after P_p was reached showing that the AISC formulas for the compression region along with that proposed by Newlin and Chen[8] are valid.

It was noted that in the column compression region, the yield pattern distribution along the toe of fillet was about 10 in. in length at a load of 620 kips and did not spread considerably until after buckling began. This agrees with the assumption made by Newlin and Chen[8] in their proposed column web formula where they assume the compression region of the column as a square web panel with dimensions $d_c \times d_c$. d_c for the W14x176 column is 11¼ in.

In Fig. 5 a prediction curve of the test is shown. P_p was determined as described in Appendix 1. Deflection in the elastic range was predicted by assuming the connection as a cantilever fixed at column centerline. Deflection of the cantilever due to bending was 0.148 in., and that due to shear of a rectangular section with area A_w was 0.128 in., giving a total predicted deflection δ_p of 0.276 in. This simple approximation gives a fairly good description of the load-deflection behavior. The ductility factor based on deflection is 13.2.

Figure 23 shows the load-rotation curve as determined from the level bars attached near juncture. Plots of the two level bars were nearly identical. As seen from this plot and the load-deflection curve of Fig. 5, the connection is able to attain P_p and rotate inelastically through a large angle. This follows curve A of Fig. 1 and thus gives a desirable type of connection for use in plastic design.

5. SUMMARY AND CONCLUSIONS

Although this test will be used in conjunction with several others to develop a better understanding of connection behavior and design, some important concepts and testing procedures can still be noted.

1. This type of connection can be used in plastic design as the plastic limit load, sufficient rotation capacity, and adequate elastic stiffness are developed. The AISC Specification provides adequate rules in design of such welded connections.
2. Elastic behavior is observed up to working load.
3. Lateral deformation of the column web in the compression region provides the cause of unloading.
4. Failure of the connection was due to a combination of excessive column web deformation in the compression region and fracture of weld at tension flange.
5. The web buckling formula proposed by Newlin and Chen[8] was shown to be accurate.
6. Applying present weld inspection procedures, no premature welding failure occurs.
7. Further studies should be made concerning possible column flange lamina tearing at welded beam flange juncture region (when load is applied perpendicular to direction of rolling of material).

6. ACKNOWLEDGMENTS

This study has been carried out as part of the research project "Beam-to-Column Connections" being conducted at Fritz Engineering Laboratory, Department of Civil Engineering, Lehigh University. Professor L. S. Beedle is Director of the Laboratory and Professor D. A. VanHorn is Chairman of the Department.

The project is sponsored jointly by the American Iron and Steel Institute and the Welding Research Council (AISI 137). Research work is carried out under the technical advice of the Welding Research Council Task Group, of which Mr. J. A. Gilligan is Chairman.

The authors wish to thank Messrs. J. A. Gilligan, O. W. Blodgett, C. F. Diefenderfer, W. E. Edwards and C. L. Kreidler for their suggestions and assistance in the fabrication of the specimens.

Thanks are also extended to Messrs. H. T. Sutherland, J. Laurinitis, and A. K. Puri for their help on instrumentation; to Mr. Richard Sopko for the photography; to Mr. Jack Gera and Mrs. Sharon Balogh for the drafting; to Miss Shirley Matlock for typing the manuscript; and to Mr. K. R. Harpel and the Laboratory Technicians for their assistance in preparing the specimen for testing.

7. APPENDICES

APPENDIX 1: DESIGN OF CONNECTION C12

(W27x94 beam and W14x176 column)

1. Determine beam span.

Plastic Moment

$$M_p = F_y Z_x = (55K/in.^2)(278\ in.^3) = 15290\ kip\text{-}in.$$

Design Ultimate Shear

Design from test C2 (Ref. 6): 7-1" A490-X bolts in single shear, $V = 7(1.7)(0.7854\ in.^2)(40K/in.^2) = 374K$. [See Ref. 5 for explanation of 40 ksi allowable shear stress.]

Check: $V_p = (F_y/\sqrt{3})\ t_w\ d_w = (55/\sqrt{3})(0.490)(25.416) = 395\ K$

$V/V_p = 374/395 = 94.7\%$

also, $V_u \leq 0.55\ F_y\ td = (0.55)(55K/in.^2)(0.490\ in.)(26.91\ in.)$

$= 399\ K \approx V_p$ O.K. [AISC, 2.5-1]

Beam Span

$$L = M_p/V = 15290\ K\text{-}in./374\ K = 40.8\ in.$$

Use 41 in. length (3'-5")

2. Select groove welds.

To conform to field practice, TC-U4 joints are used. The bevel angle and root opening for beam flange groove welds are 30^o and 3/8 in., and for beam web groove welds are 45^o and $\frac{1}{4}$ in.

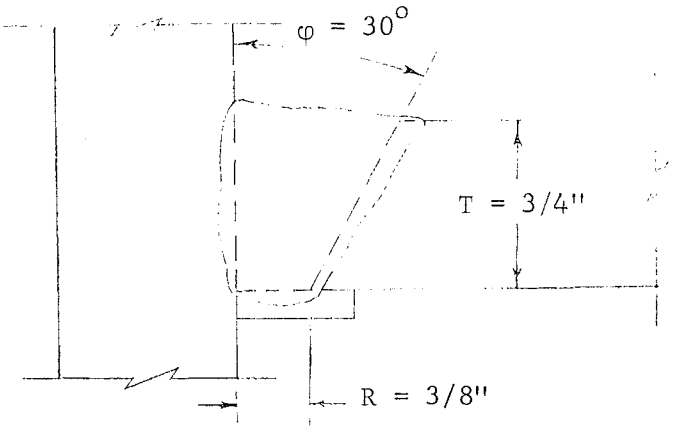

for flanges

For web, use $\varphi = 45^{\circ}$, R = ¼".

3. Check horizontal stiffener requirements.

Opposite compression flange:

Using AISC Specification,

$$t < \frac{C_1 A_f}{t_b + 5k} \qquad \text{[AISC, 1.15-1]}$$

$$t < \frac{(1)(9.990 \text{ in.})(0.747 \text{ in.})}{0.747 \text{ in.} + 5\ (2.0 \text{ in.})} = 0.694 \text{ in.}$$

t for W14x176 column is 0.820 in. ∴ O.K.

$$t \leq \frac{d_c \sqrt{F_y}}{180} \qquad \text{[AISC, 1.15-2]}$$

$$t \leq \frac{(15.25 \text{ in.} - 4.00 \text{ in.})\sqrt{55 \text{ K/in}^2}}{180} = 0.464 \text{ in.} < 0.820 \text{ in.} \quad \text{O.K.}$$

Using Fritz Engineering Laboratory Report 333.14[8],

$$t \leq \frac{d_c^2 \sqrt{F_y} + 180\ C_1 A_f}{125\ d_c \sqrt[4]{F_y}}$$

$$t \leq \frac{(11.25 \text{ in.})^2 \sqrt{55 \text{ K/in.}^2} + 180\ (1)(9.990 \text{ in.})(0.747 \text{ in.})}{125\ (11.25 \text{ in.}) \sqrt[4]{55 \text{ K/in.}^2}}$$

$$= 0.596 \text{ in.} < 0.820 \text{ in.} \quad \therefore \text{O.K.}$$

Stiffeners are not required opposite the compression flange.

Opposite tension flange:

$$t_f < 0.4\sqrt{C_1 A_f} \quad \text{[AISC, 1.15-3]}$$

$$t_f < 0.4\sqrt{(1)(9.990 \text{ in.})(0.747 \text{ in.})} = 1.092 \text{ in.}$$

t_f for W14x176 column is 1.313 in.; therefore stiffeners not required.

Note: Since for a wide-flange section most of the bending moment is taken by the flanges, it is an usual practice to assume that the flange force $T = M_p/d$. An equivalent flange area can be written as

$$A_f' = T/F_y = M_p/(F_y d) = Z_x/d$$

The AISC Formula (1.15-3) becomes

$$t_f < 0.4\sqrt{C_1(Z_x/d)}$$

Substituting for section properties of W27x94, the required minimum column flange thickness is

$$t_f < 0.4\sqrt{(1)(278/26.91)} = 1.284 \text{ in.}$$

The least column size providing t_f greater than 1.284 in. is W14x176 with $t_f = 1.313$ in.

4. Select erection plates.

The size of the erection plate used is 3/8" x 4" x 23½", which conforms to common practice. The plate was tack welded to the column flange to serve as a backing strip for beam web groove weld. Two 3/4" diameter A307 bolts were used to fasten the plate to beam web.

APPENDIX 2: STRESS-STRAIN RELATIONSHIP

1. For Strain Rosettes

(a) Tension or Compression

Using the Von Mises yield criterion, the effective stress is defined as

$$\sigma_e = \frac{1}{\sqrt{2}} \left[(\sigma_1-\sigma_2)^2 + (\sigma_2-\sigma_3)^2 + (\sigma_3-\sigma_1)^2 + 6(\tau_{12}^2 + \tau_{23}^2 + \tau_{31}^2)\right]^{1/2}$$

The effective strain is defined as

$$\epsilon_e = \frac{\sqrt{2}}{2(1+\mu)} \left[(\epsilon_1-\epsilon_2)^2 + (\epsilon_2-\epsilon_3)^2 + (\epsilon_3-\epsilon_1)^2 + 6(\epsilon_{12}^2 + \epsilon_{23}^2 + \epsilon_{31}^2)\right]^{1/2}$$

For a simple tension test,

$\sigma_2 = \sigma_3 = \tau_{12} = \tau_{23} = \tau_{31} = 0$, $\epsilon_{12} = \epsilon_{23} = \epsilon_{31} = 0$, and $\epsilon_2 = \epsilon_3 = -\mu\epsilon_1$

These equations reduce to $\sigma_e = \sigma_1$ and $\epsilon_e = \epsilon_1$, respectively.

($\sigma_1 = \sigma_y$ and $\epsilon_1 = \epsilon_y$ from tensile tests) (See Ref. 4)

From linear elasticity,

$$\epsilon_x = \frac{1}{E}\left[\sigma_x - \mu\,(\sigma_y + \sigma_z)\right]$$

$$\epsilon_y = \frac{1}{E}\left[\sigma_y - \mu\,(\sigma_x + \sigma_z)\right]$$

$$\epsilon_z = \frac{1}{E}\left[\sigma_z - \mu\,(\sigma_x + \sigma_y)\right]$$

For the connection web portions, assume plane stress condition, i.e. $\sigma_z = 0$. Therefore,

$$\epsilon_z = -\frac{\mu\,(\epsilon_x + \epsilon_y)}{(1-\mu)}$$

$$\sigma_x = \frac{(1-\mu)\,E}{(1+\mu)(1-2\mu)}\,\epsilon_x + \frac{\mu\,E}{(1+\mu)(1-2\mu)}\,(\epsilon_y + \epsilon_z)$$

$$\sigma_y = \frac{(1-\mu)\,E}{(1+\mu)(1-2\mu)}\,\epsilon_y + \frac{\mu\,E}{(1+\mu)(1-2\mu)}\,(\epsilon_x + \epsilon_z)$$

(b) Shear

For cases of high shear, the effective stress and strain equations reduce to

$$\sigma_e = \sqrt{3}\ \tau_{12}$$

$$\epsilon_e = \frac{\sqrt{3}}{2\ (1 + \mu)}\ \gamma_{12}$$

where $\gamma_{12} = 2\ \epsilon_{12}$.

(c) Shear and Axial Stresses in Panel Zone

From Ref. 4, for high shear and axial stresses in a connection panel, the effective stress and effective strain are:

$$\sigma_e = \frac{1}{\sqrt{2}} \left[2\ \sigma_1^2 + 6\ \tau_{12}^2\right]^{1/2}$$

$$\epsilon_e = \frac{\sqrt{2}}{2\ (1 + \mu)} \left[2\ (1 + \mu)^2\ \epsilon_1^2 + \frac{3}{2}\ \gamma_{12}^2\right]^{1/2}$$

Using either Mohr's circle for stress and comparing the principal stresses to the appropriate effective stress, or Mohr's circle for strain and comparing the principal strains to the appropriate effective strain, yielding at the strain rosette can be determined.

It was found that by neglecting ϵ_z results of rosette stresses changed insignificantly so that in future tests, data could be analyzed considering only a two-dimensional system.

In determining γ_{12} from the strain rosette,

$$\gamma_{12} = \epsilon_1 + \epsilon_2 - 2\epsilon_b$$

$$\tau_{xy} = G\gamma_{12}$$

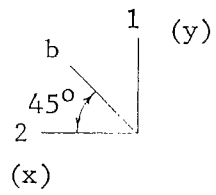

2. For 90^{o} Gages

The effective stress used was $\sigma_e = \sigma_1$ (where $\sigma_1 = \sigma_y$ of tensile tests). Stresses in the 90^{o} gages were determined by

$$\sigma_x = \frac{E}{1 - \mu^2} (\epsilon_2 + \mu \epsilon_1)$$

$$\sigma_y = \frac{E}{1 - \mu^2} (\epsilon_1 + \mu \epsilon_2)$$

3. Linear Gages

Strain readings were compared directly to ϵ_y and ϵ_{st}. Below the elastic limit $\sigma = E\epsilon$; between ϵ_y and ϵ_{st}, $\sigma = \sigma_y$; above ϵ_{st}, $\sigma = \sigma_y + E_{st} (\epsilon - \epsilon_{st})$.

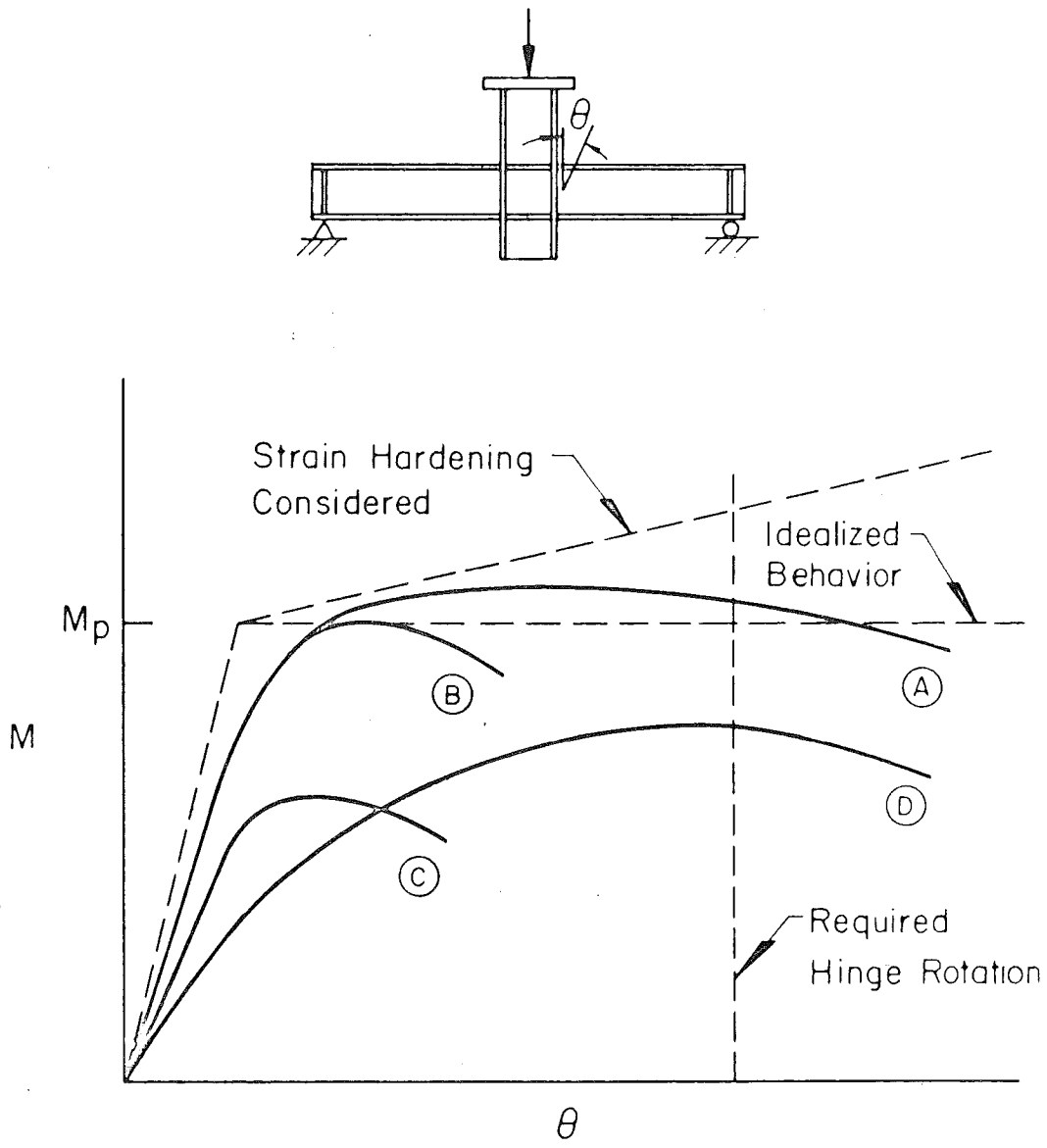

Fig. 1 Moment-rotation curves

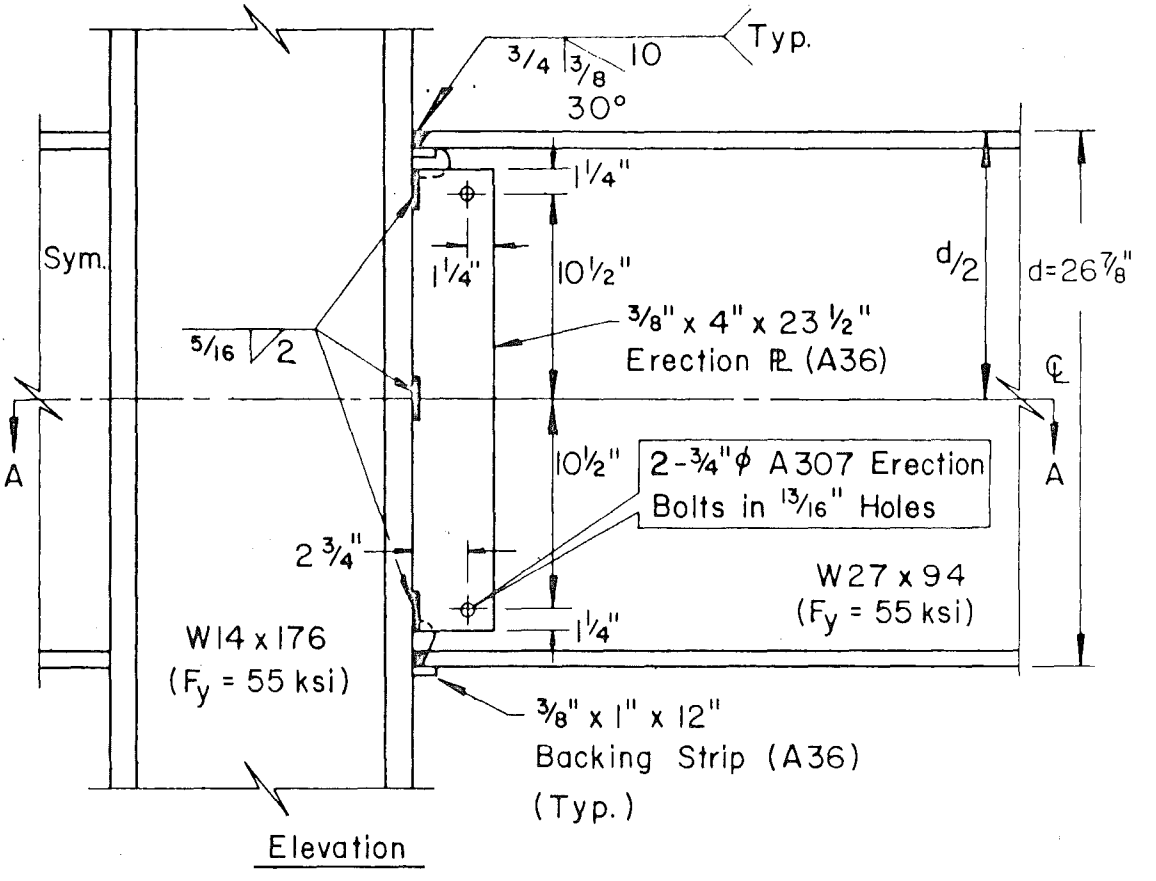

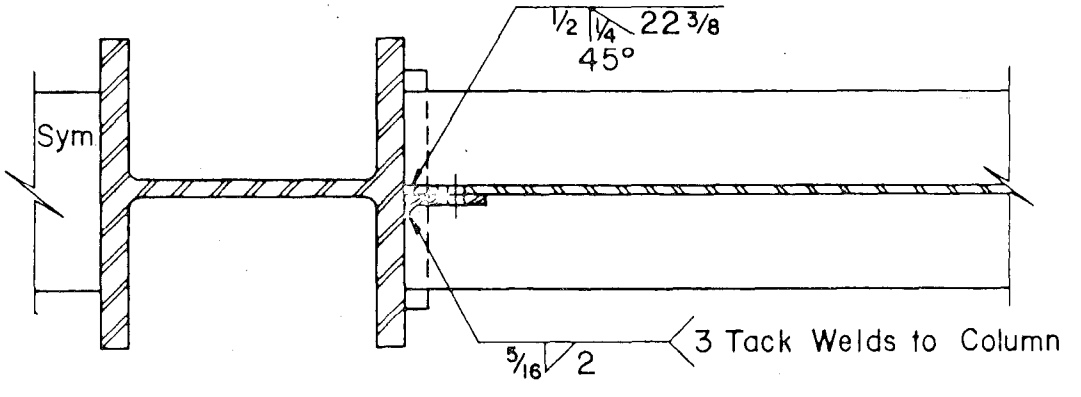

Scale:

0 5 10 in.

Fig. 2 Test C12 detail

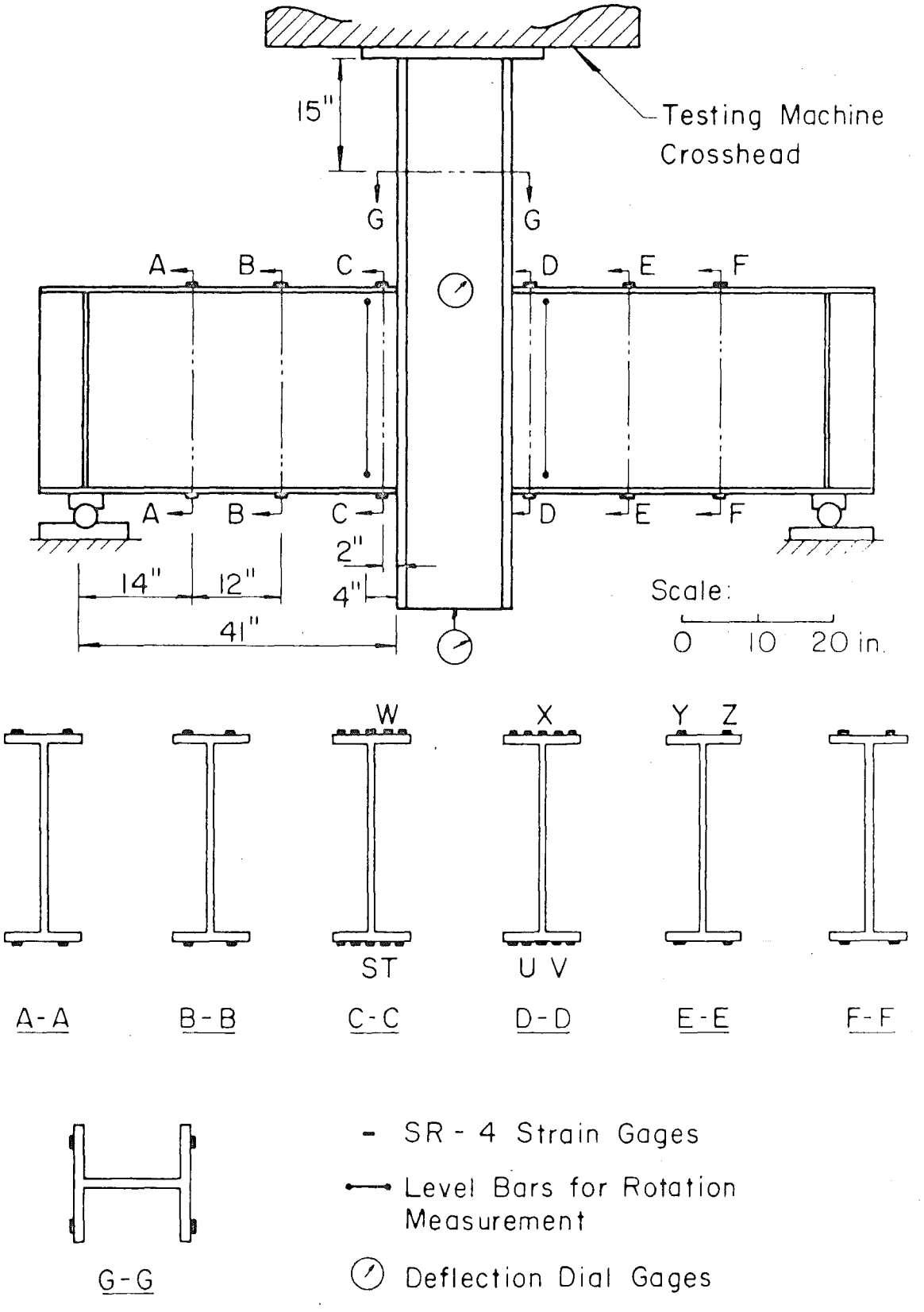

Fig. 3 General instrumentation

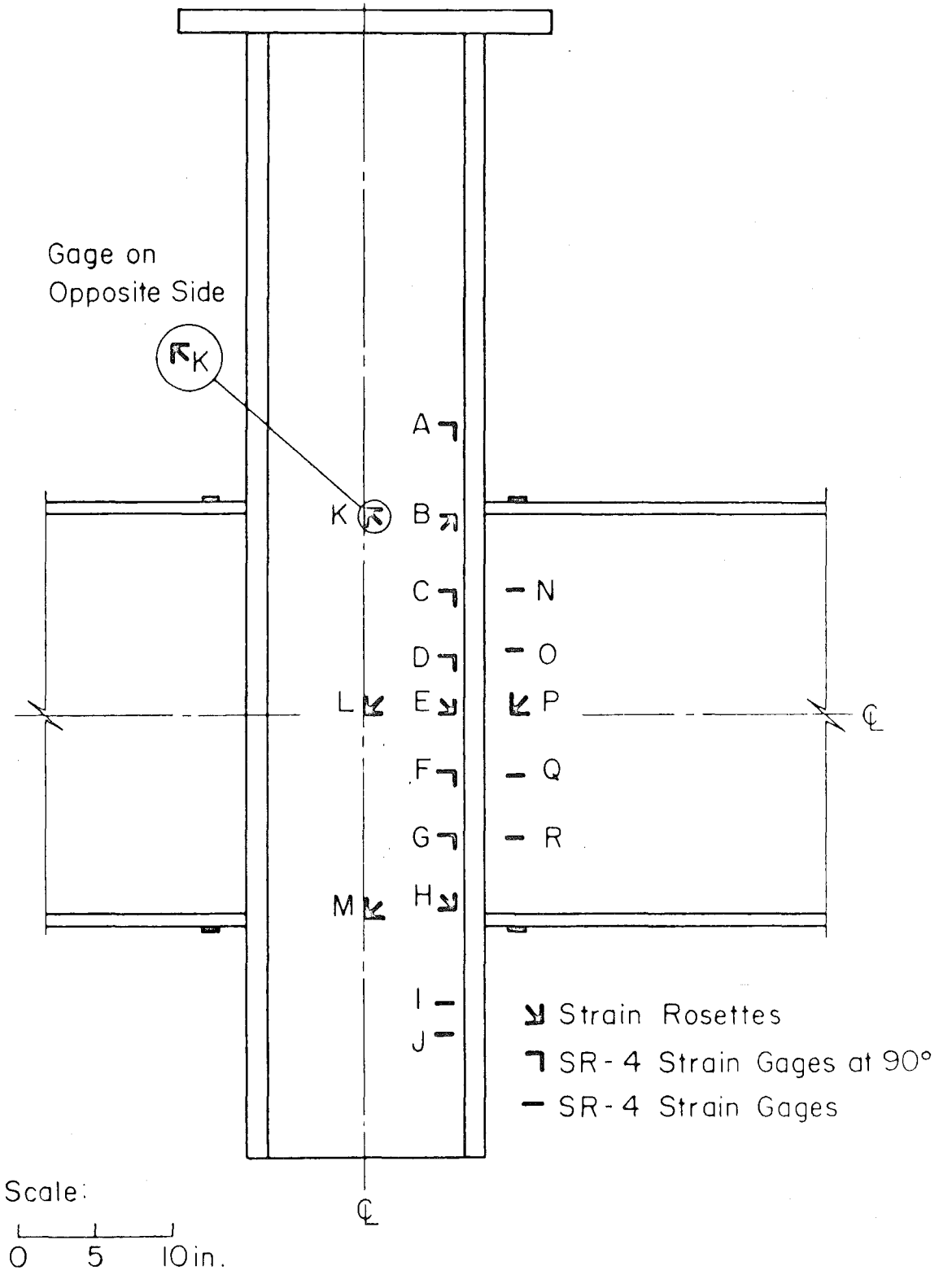

Fig. 4 Panel zone instrumentation

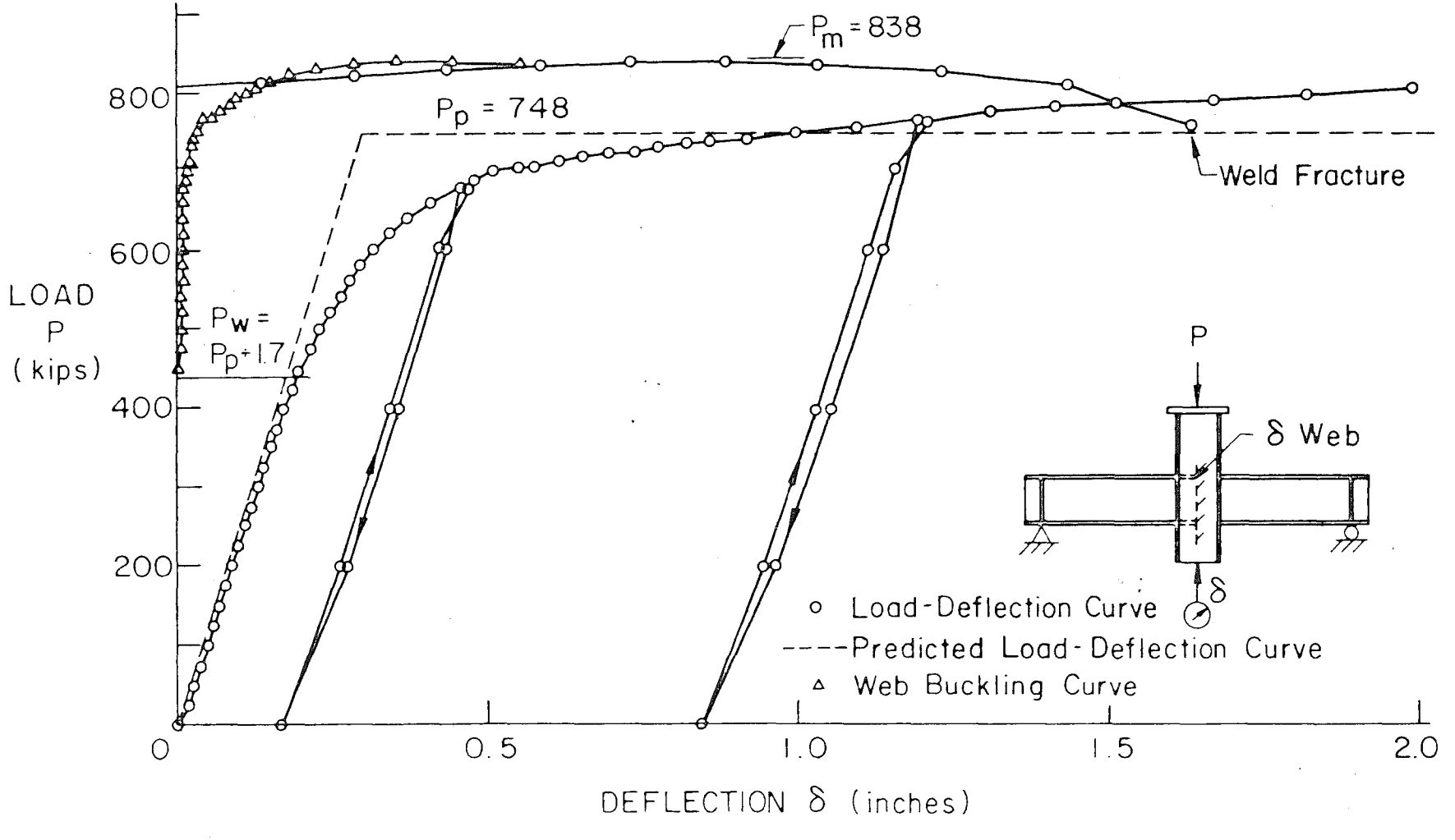

Fig. 5 Load-deflection curve

Fig. 6 Fracture of weld at tension flange

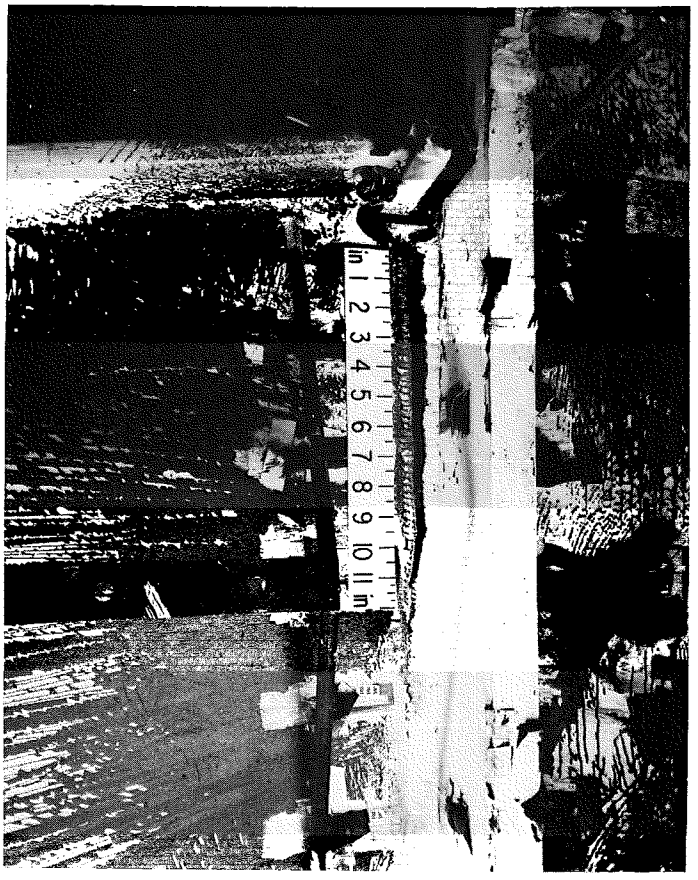

Fig. 7 Fracture of weld along beam web

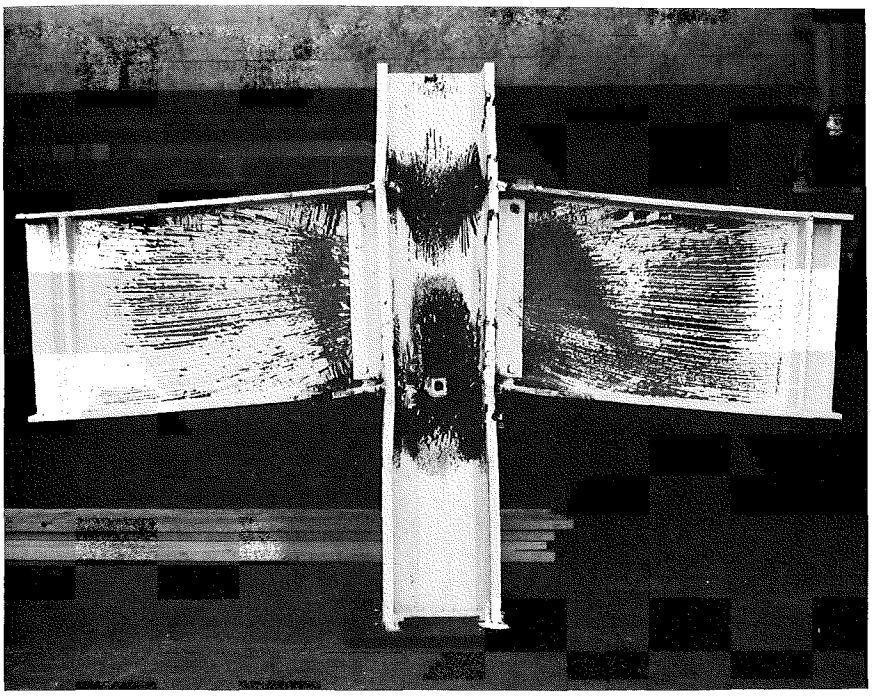

Fig. 8 Connection at end of test

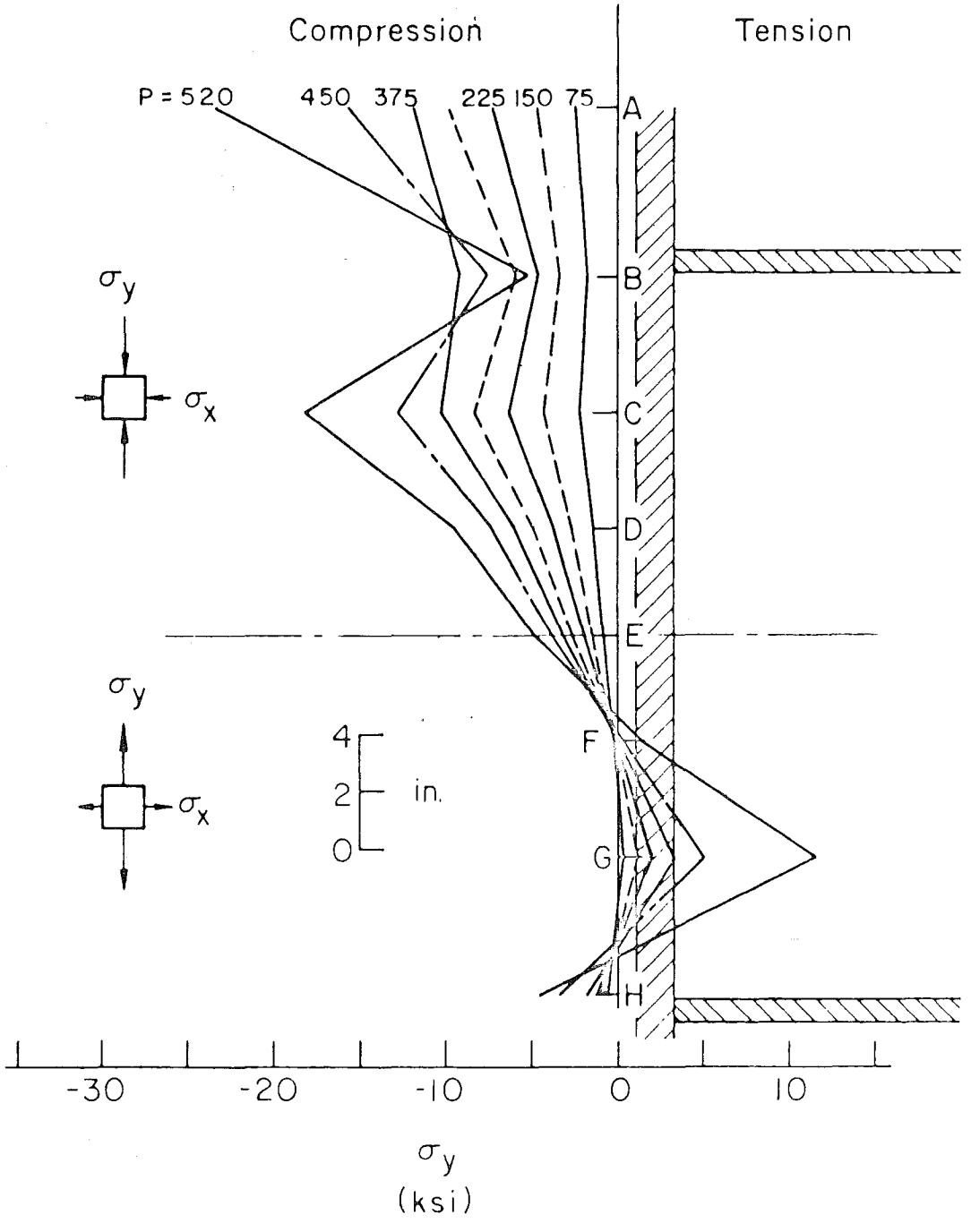

Fig. 9 Variation of vertical stress along column innerface (k-line)

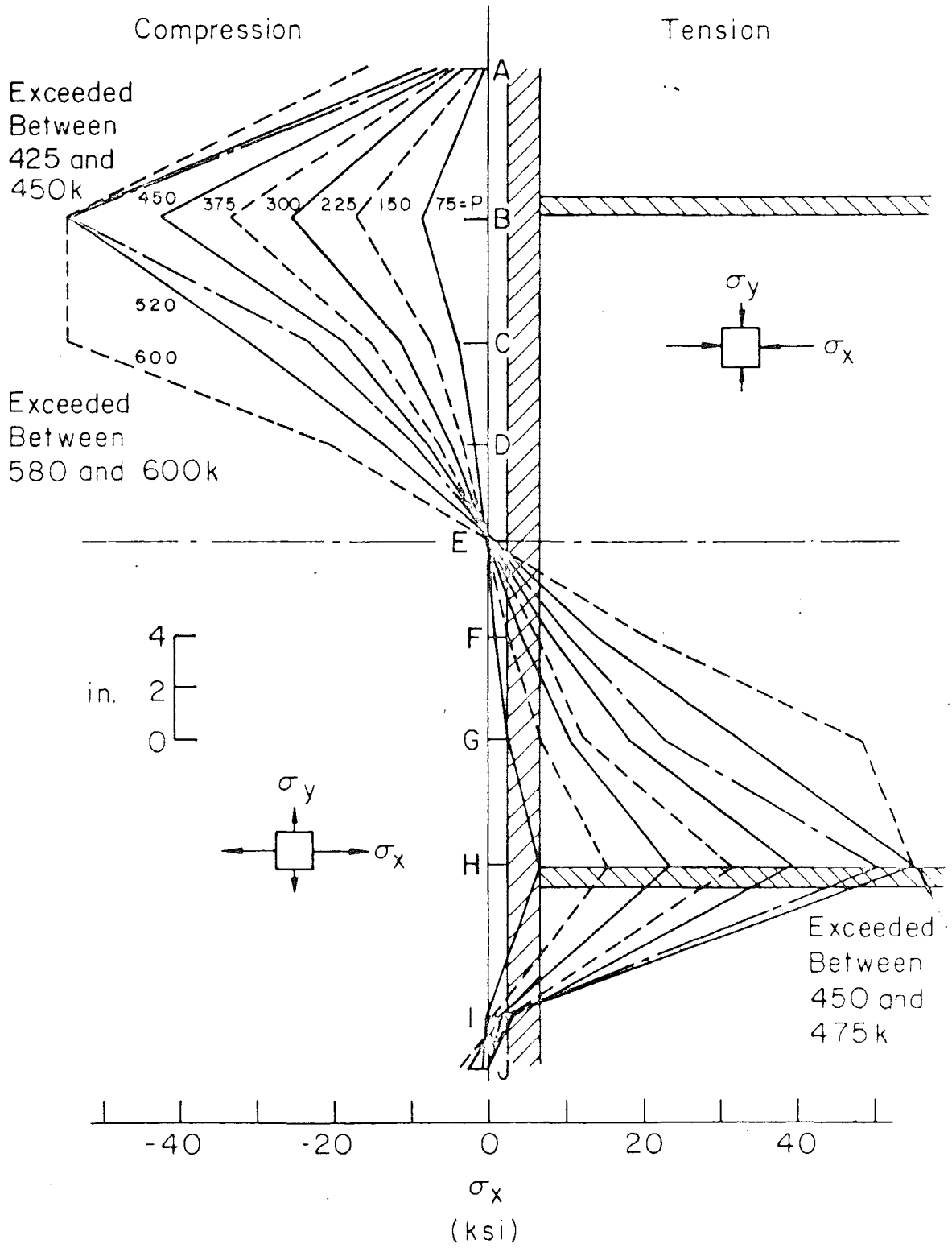

Fig. 10 Variation of horizontal stress along column innerface (k-line)

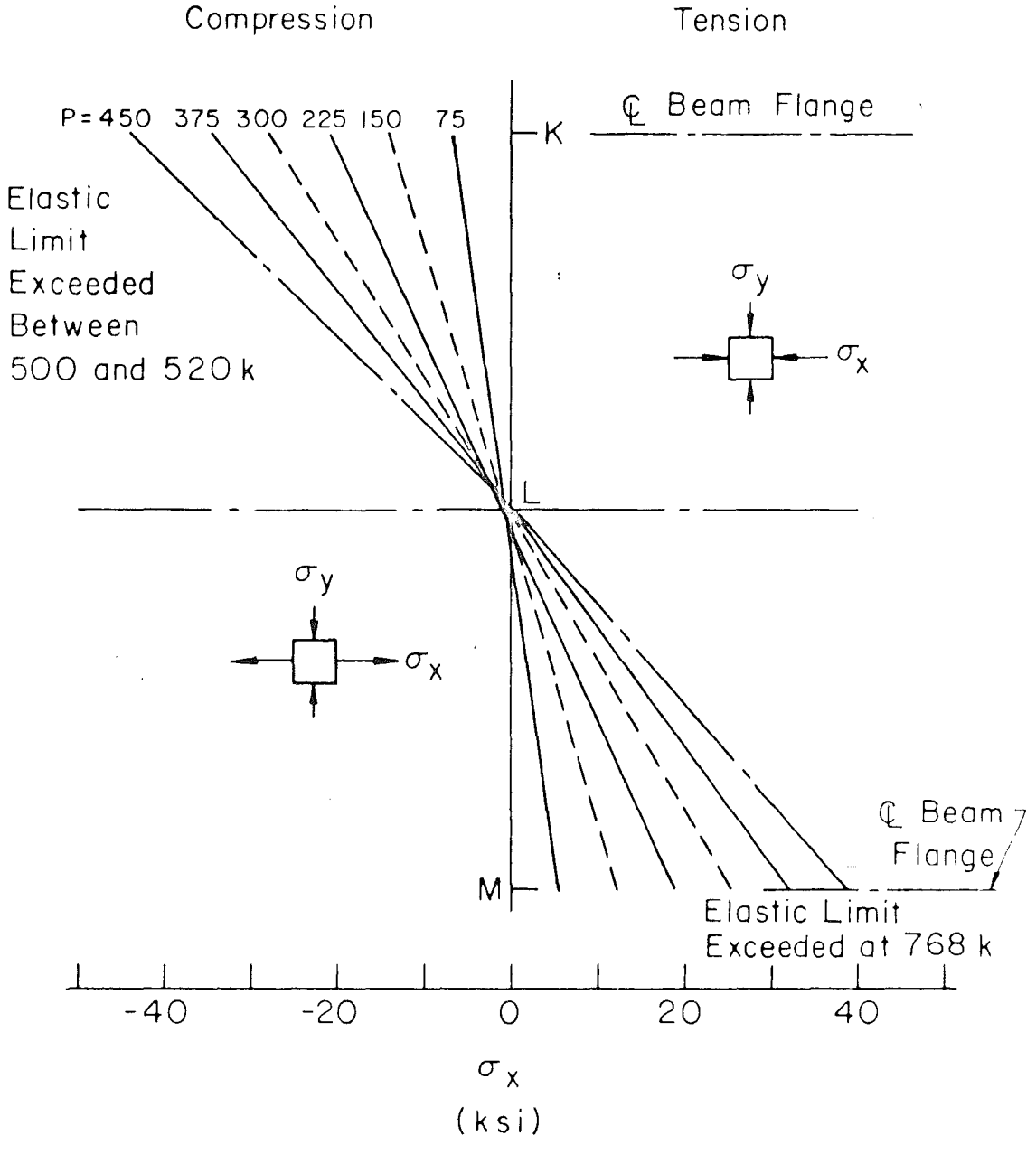

Fig. 11 Variation of horizontal stress along column centerline

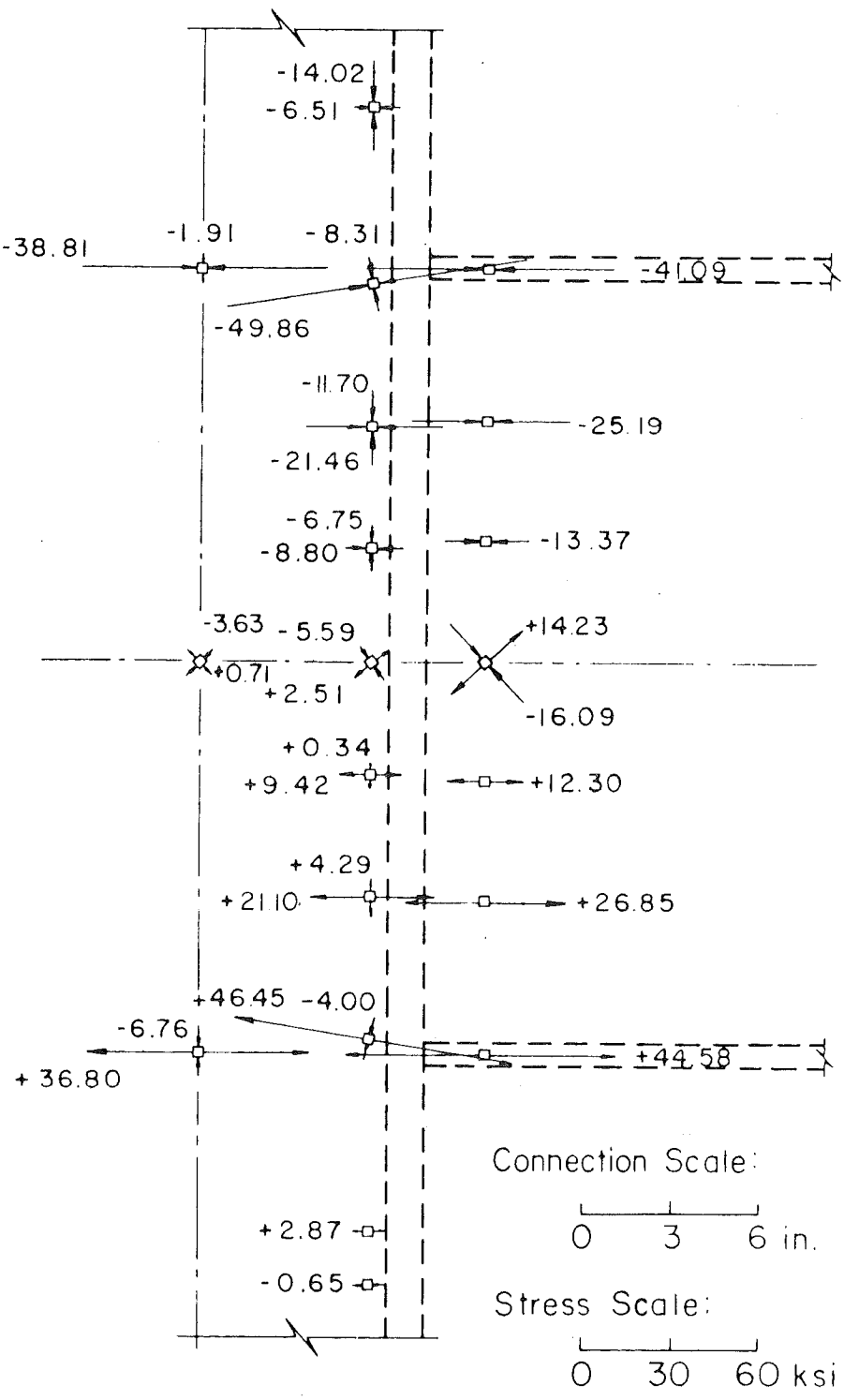

Fig. 12 Panel stress field at 425 K load

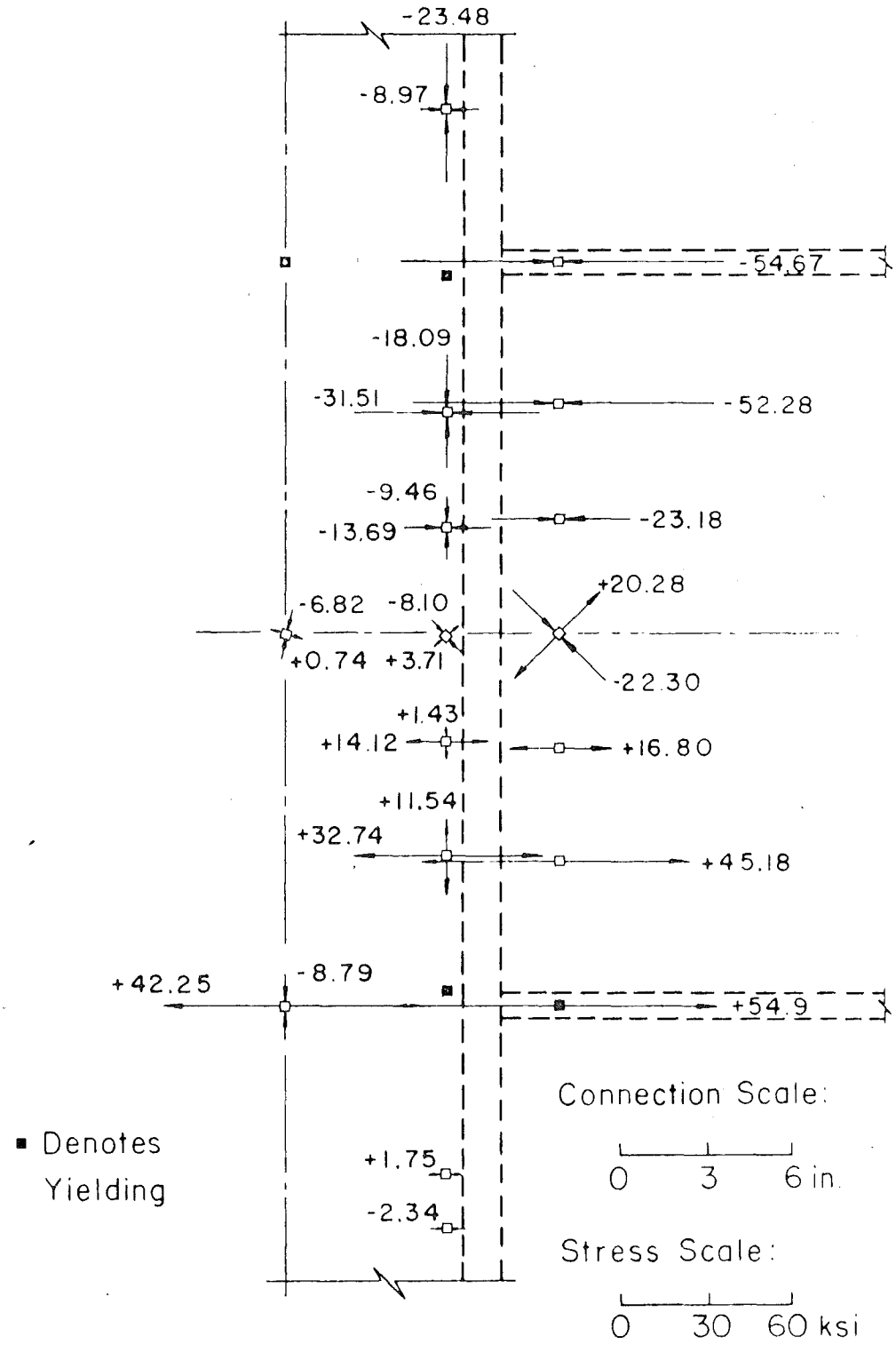

Fig. 13 Panel stress field at 520 K load

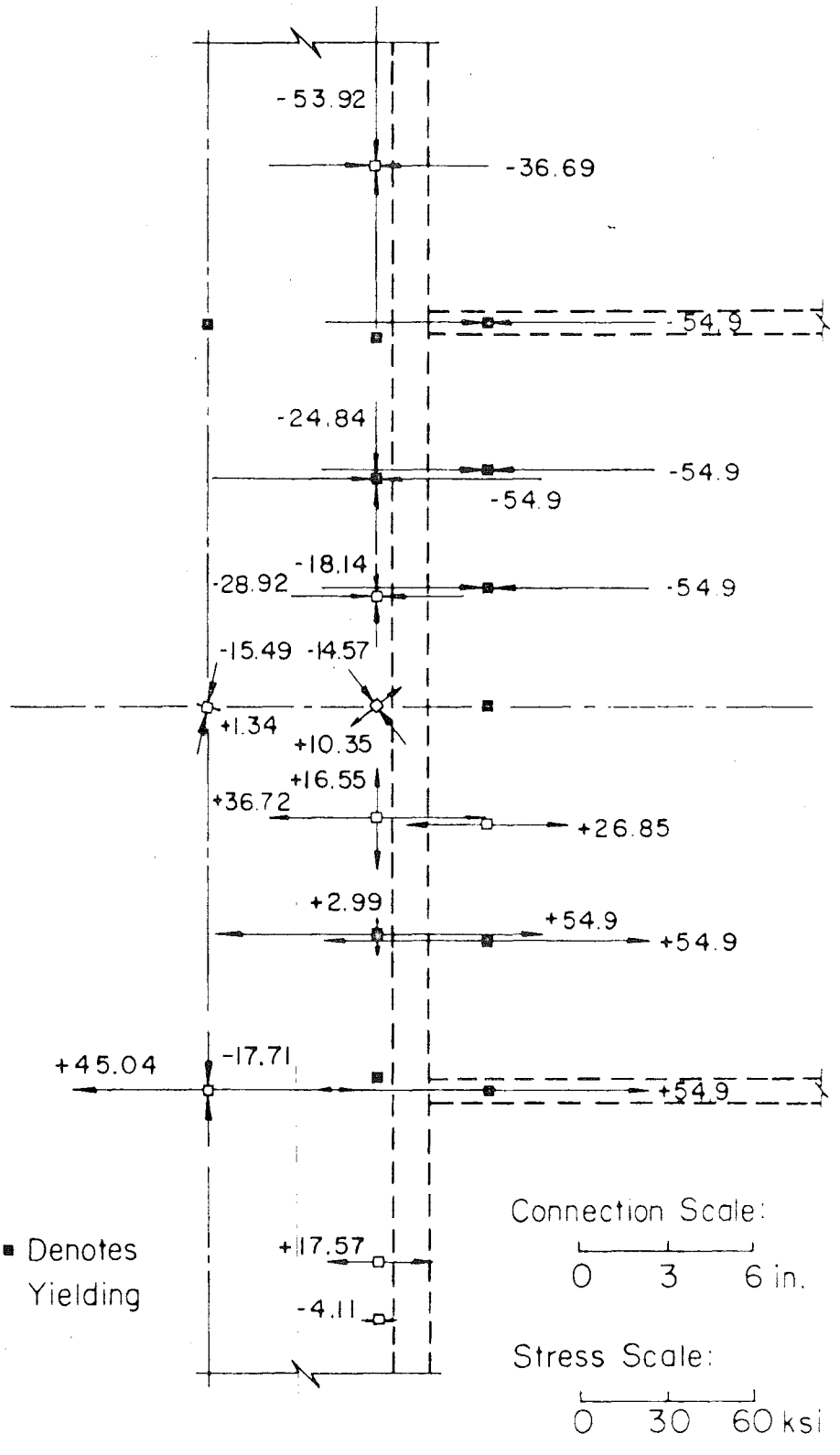

Fig. 14 Panel stress field at 680 K load

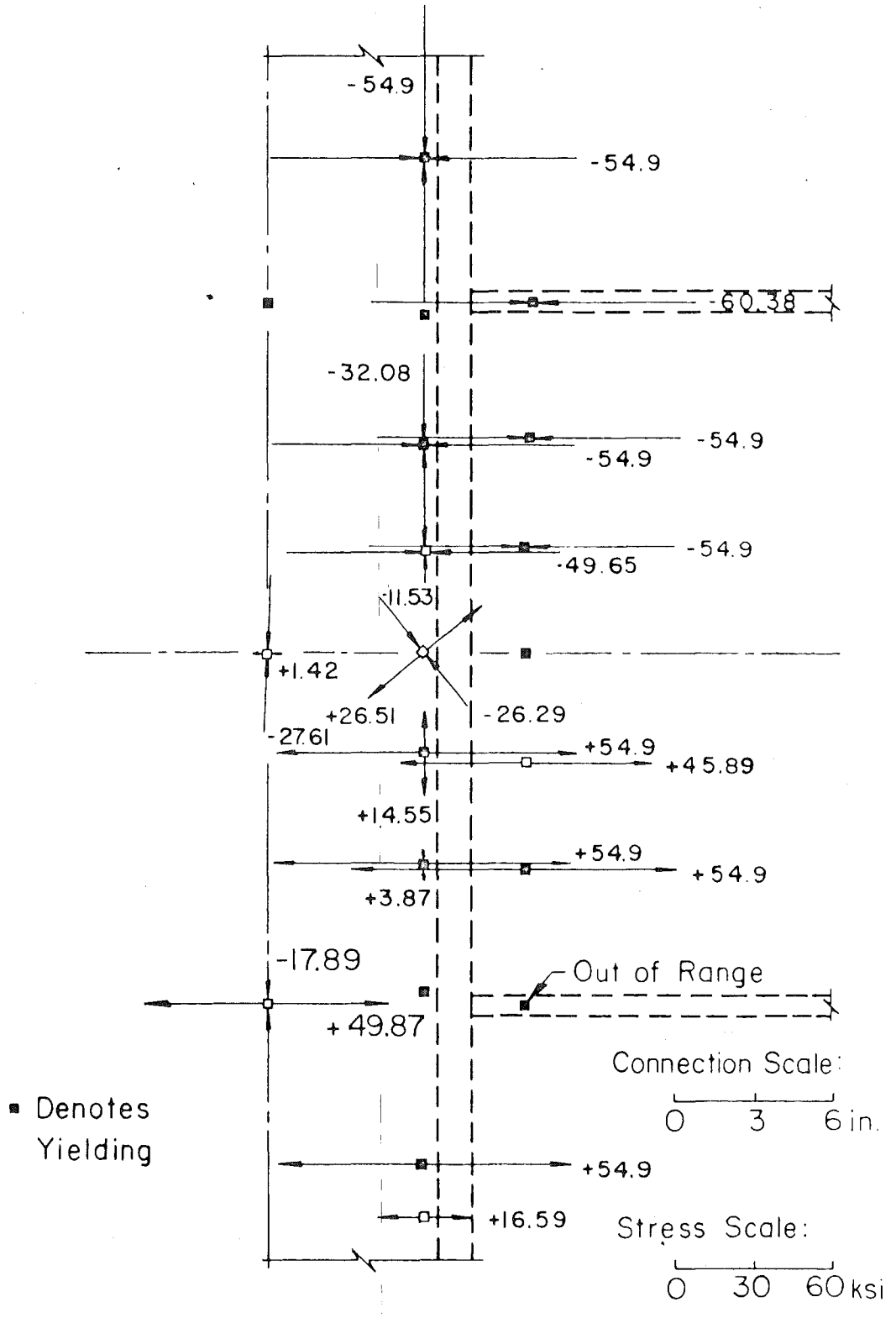

Fig. 15 Panel stress field at 750 K load

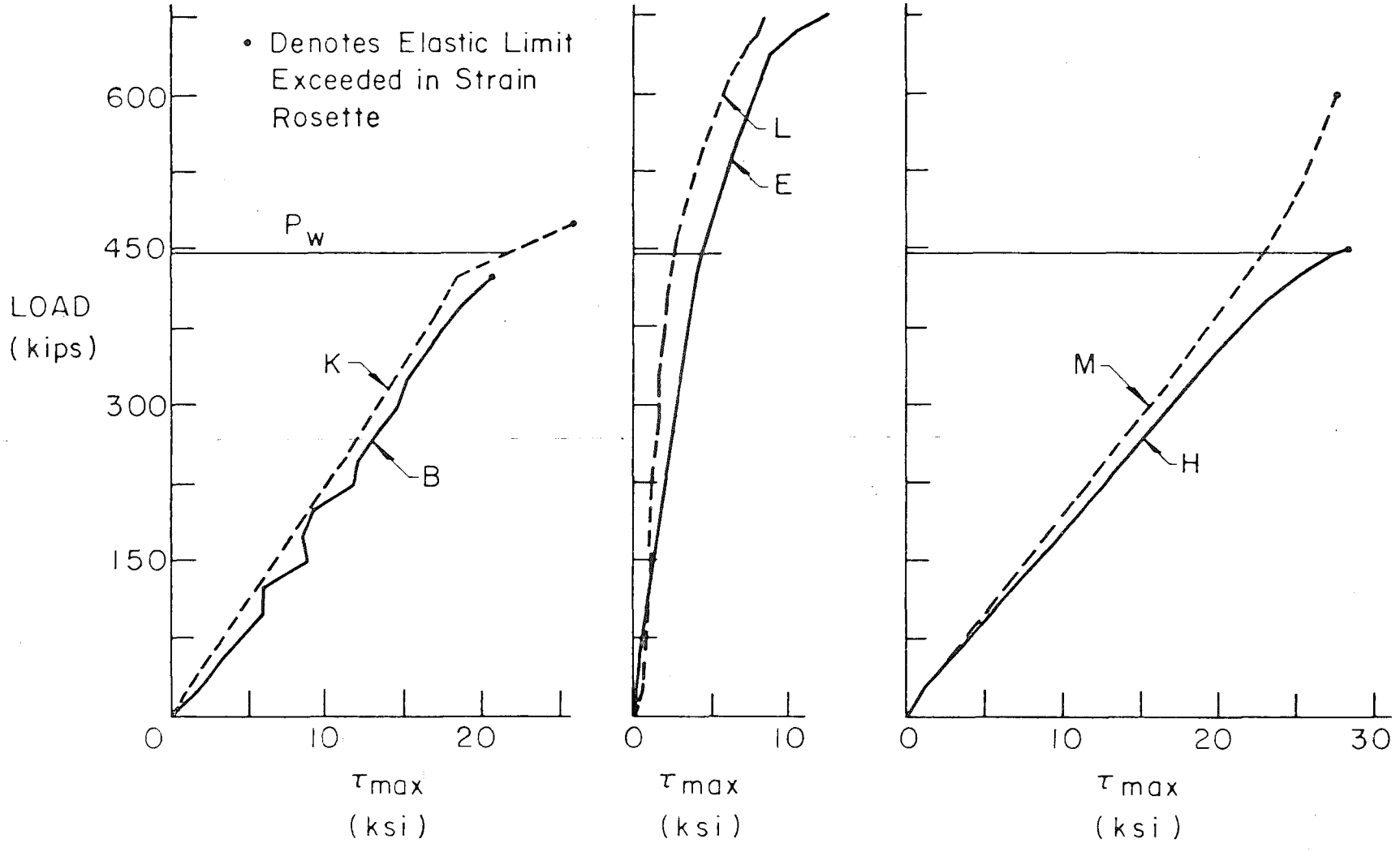

Fig. 16 Maximum shear stress variation in column web

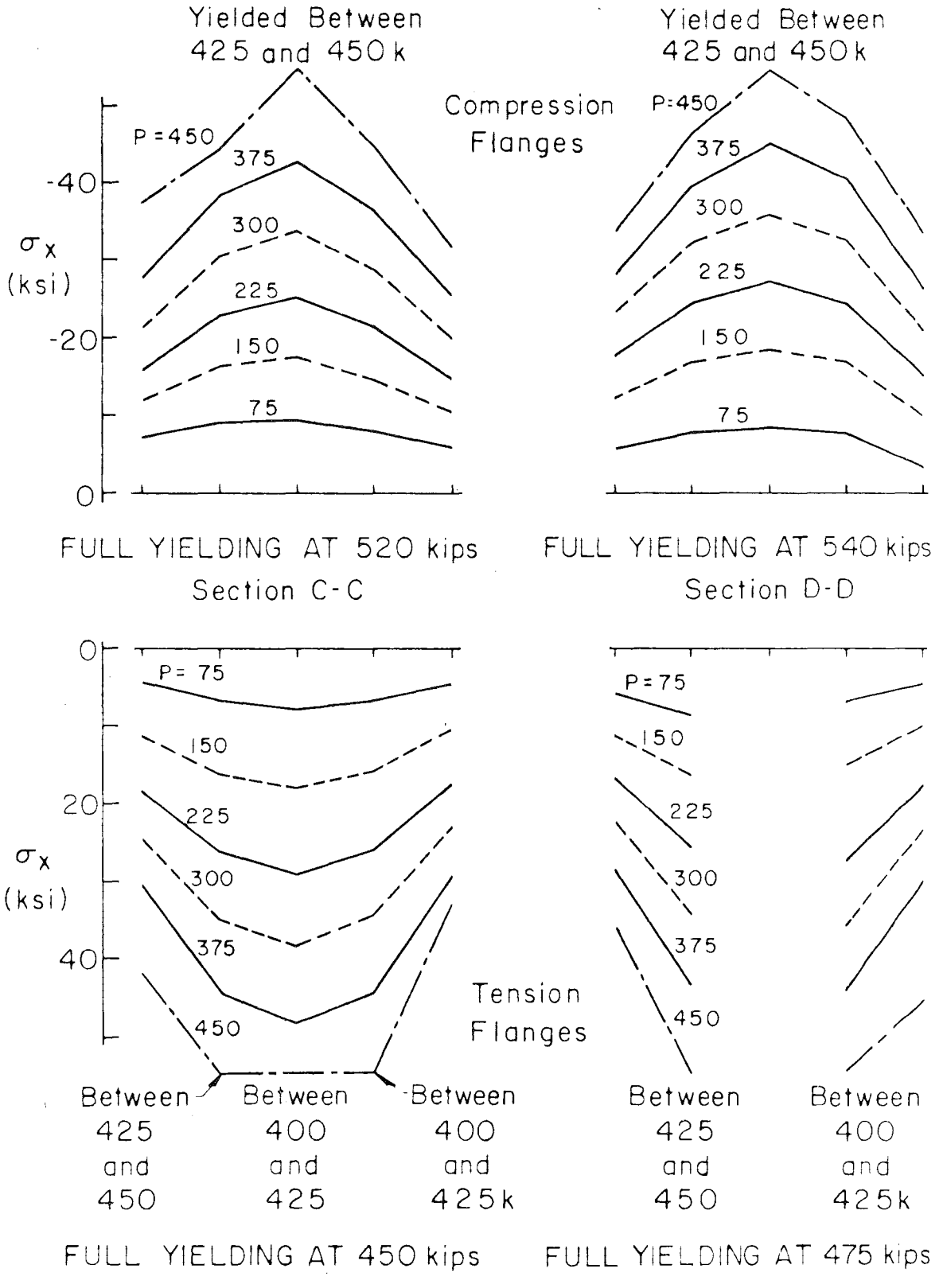

Fig. 17 Variation of stress across beam flanges adjacent to column

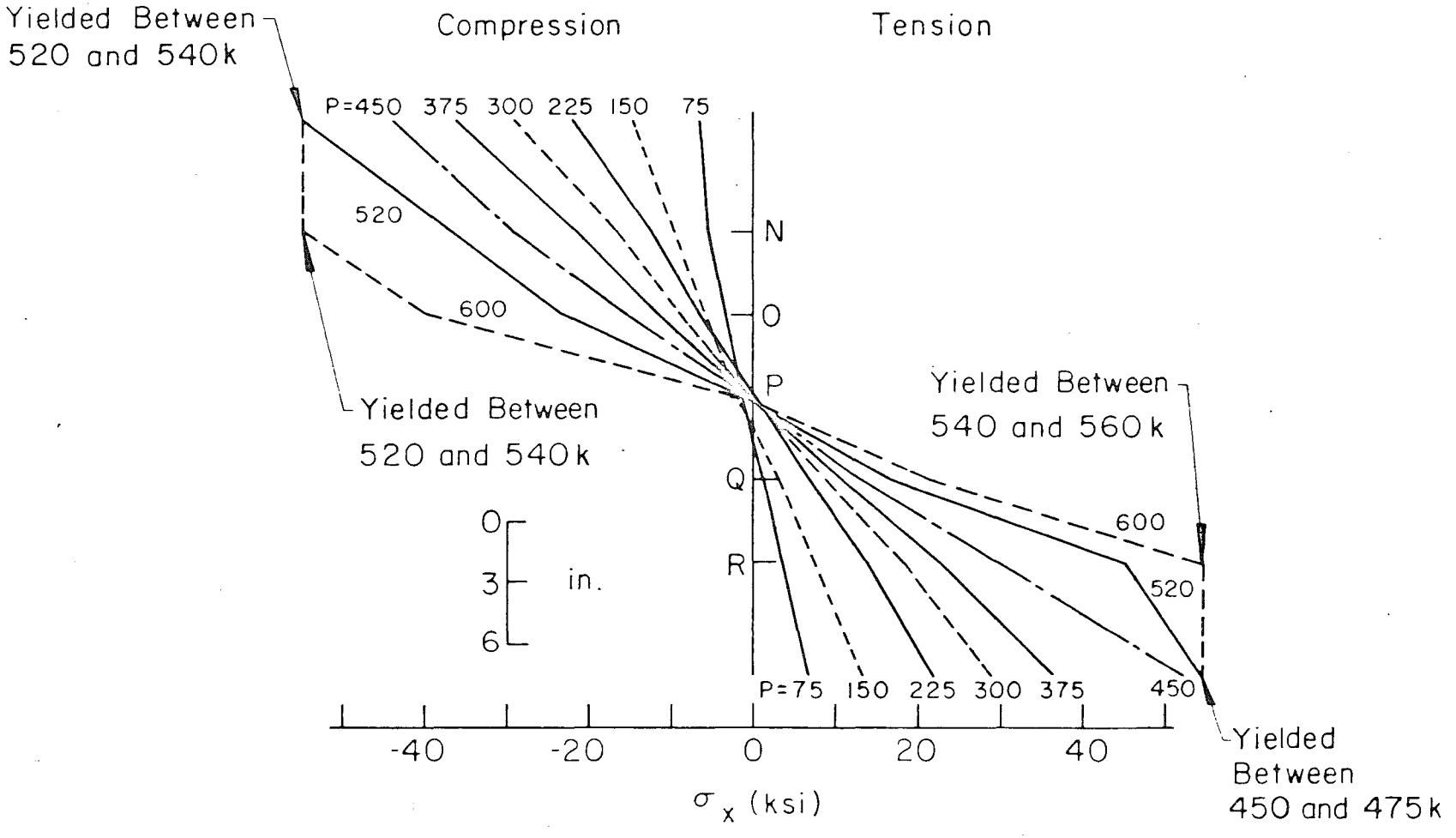

Note: All Flange Points Represent Average Flange Stress

Fig. 18 Stress variation along beam depth adjacent to column flange

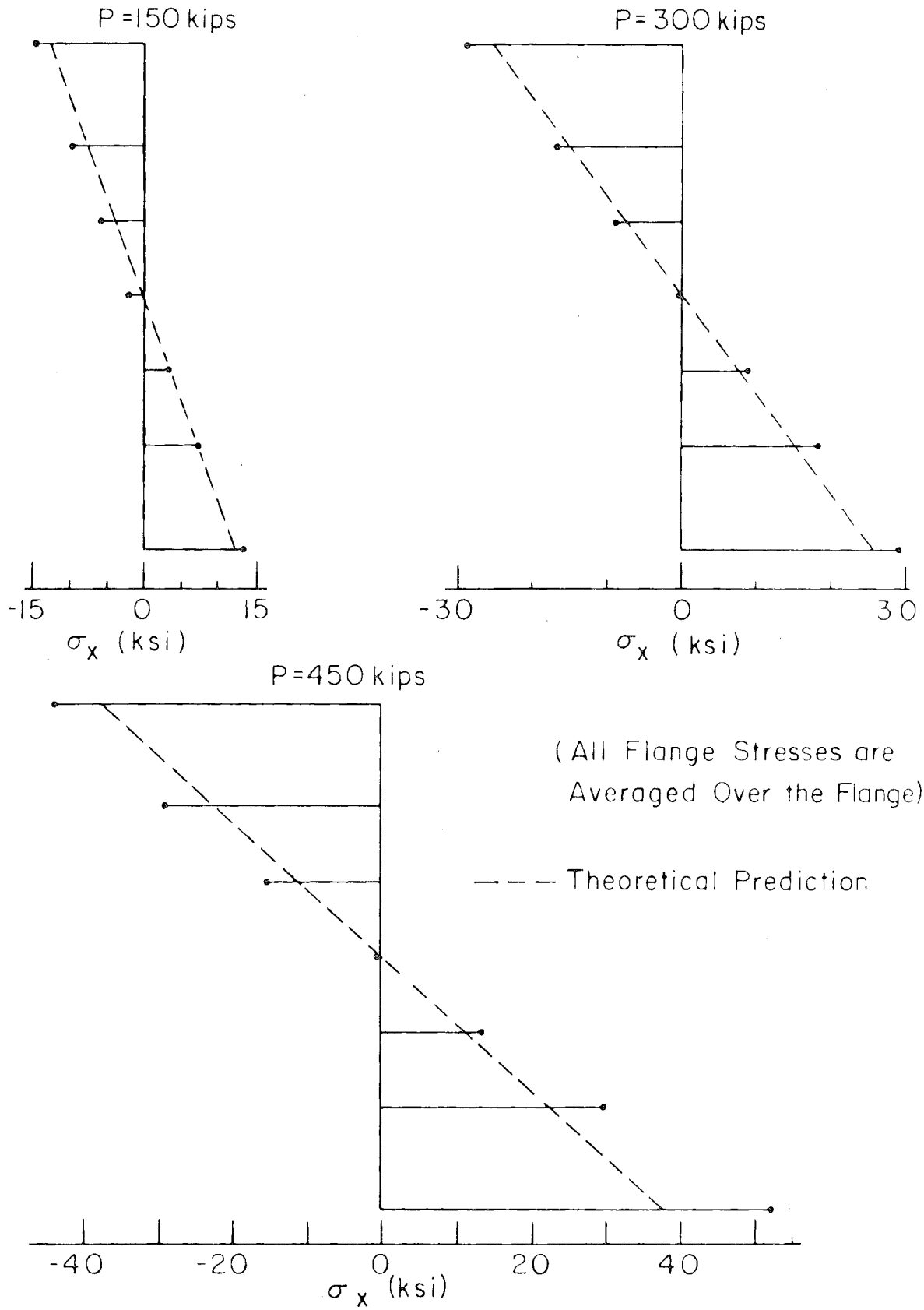

Fig. 19 Beam stress variation--predicted versus actual

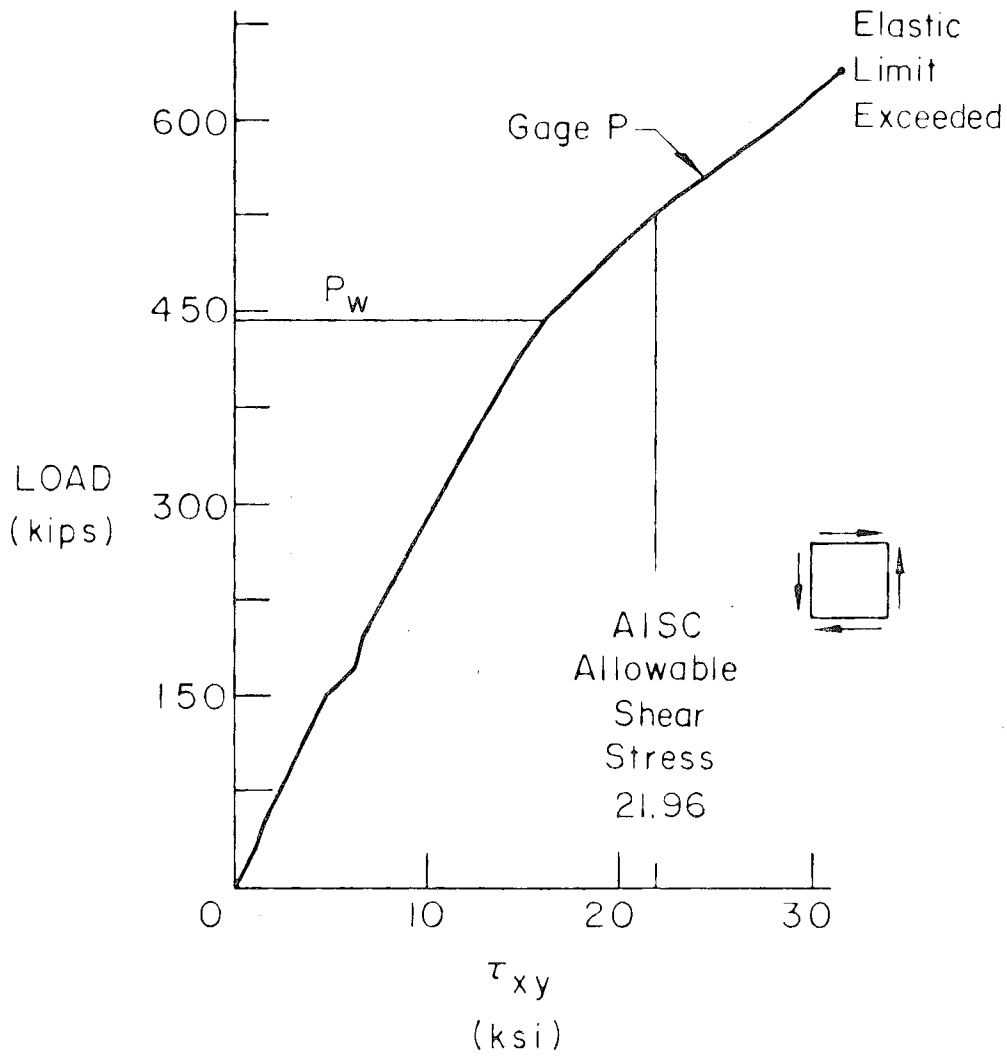

Fig. 20 Beam shear stress variation with load at section D-D

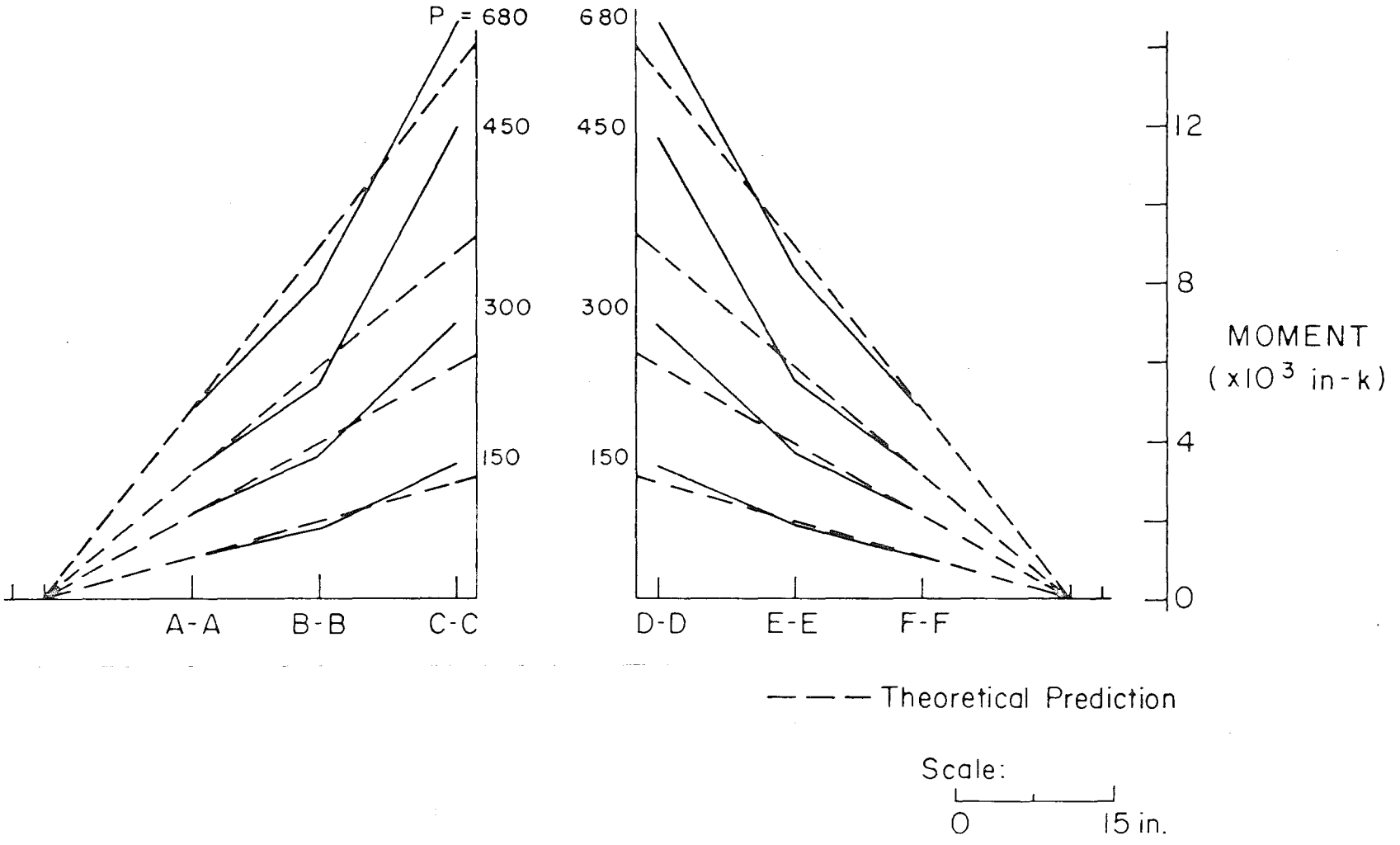

Fig. 21 Bending moment diagram

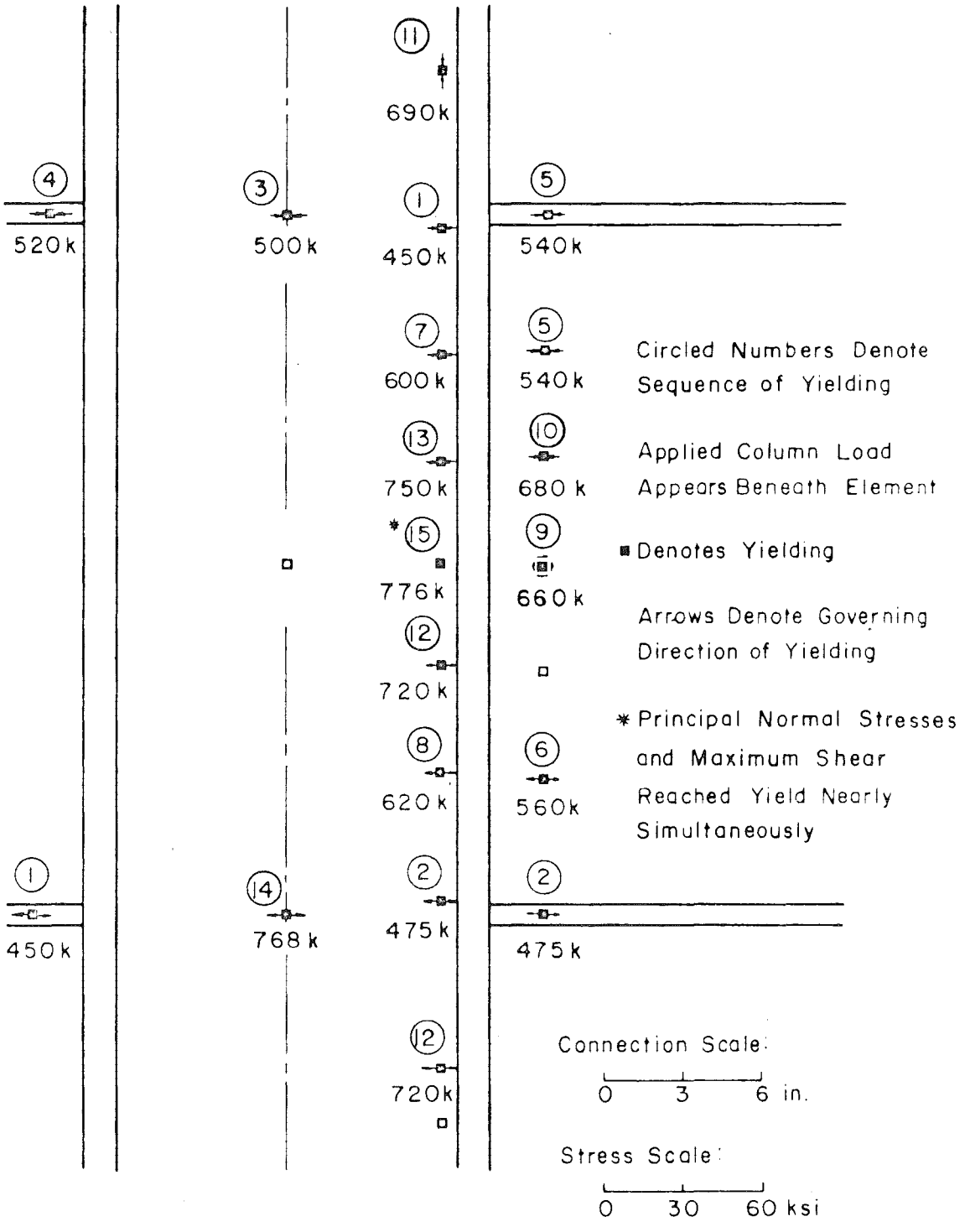

Fig. 22 Sequence of panel zone yielding

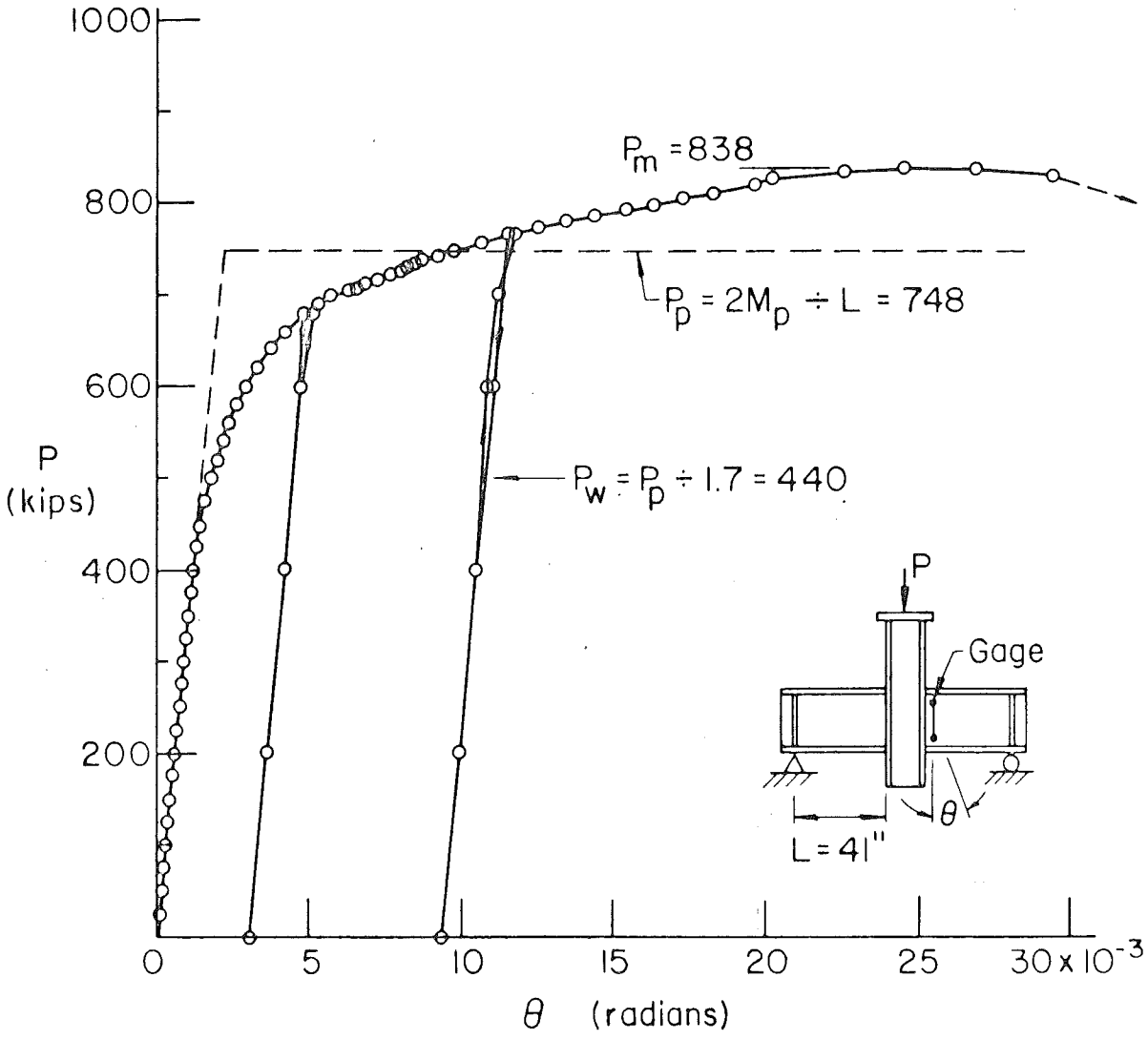

Fig. 23 Load-rotation curve

9. REFERENCES

1. AISC
MANUAL OF STEEL CONSTRUCTION, 7th ed., American Institute of Steel Construction, 1970.

2. AWS
CODE FOR WELDING IN BUILDING CONSTRUCTION, AWS D1.0-69, 9th ed., American Welding Society, 1969.

3. Beedle, L. S. and Christopher, R.
TESTS OF STEEL MOMENT CONNECTIONS, AISC Engineering Journal, 1 (4), October 1964, p. 116.

4. Fielding, D. J., Chen, W. F., and Beedle, L. S.
FRAME ANALYSIS AND CONNECTION SHEAR DEFORMATION, Fritz Laboratory Report 333.16, Lehigh University, Bethlehem, Pa., January 1972.

5. Fisher, J. W. and Beedle, L. S.
CRITERIA FOR DESIGNING BEARING-TYPE BOLTED JOINTS, ASCE Structural Division Journal, 91 (ST5), Paper No. 4511, October 1965, p. 129.

6. Huang, J. S., Chen, W. F., and Regec, J. E.
TEST PROGRAM OF STEEL BEAM-TO-COLUMN CONNECTIONS, Fritz Laboratory Report 333.15, Lehigh University, Bethlehem, Pa., July 1971.

7. Huang, J. S., Fielding, D. J., Chen, W. F., and Staff
FUTURE CONNECTION RESEARCH PROBLEMS, Fritz Laboratory Report 333.7, Lehigh University, Bethlehem, Pa., July 1972.

8. Newlin, D. E., and Chen, W. F.
STRENGTH AND STABILITY OF COLUMN WEB IN WELDED BEAM-TO-COLUMN CONNECTIONS, Fritz Laboratory Report 333.14, Lehigh University, Bethlehem, Pa., May 1971.

9. Popov, E. P. and Stephen, R. M.
CYCLIC LOADING OF FULL-SIZE STEEL CONNECTIONS, Earthquake Engineering Research Center Report 70-3, University of California, Berkeley, Calif., July 1970.

10. Regec, J. E., Huang, J. S., and Chen, W. F.
MECHANICAL PROPERTIES OF C-SERIES CONNECTIONS, Fritz Laboratory Report 333.17, Lehigh University, Bethlehem, Pa., April 1972.